energies

MDPI

Article

Synthesis of Biobased Composite Heterogeneous Catalyst for Biodiesel Production Using Simplex Lattice Design Mixture: Optimization Process by Taguchi Method

Christopher Tunji Oloyede [1,*], Simeon Olatayo Jekayinfa [1], Abass Olanrewaju Alade [2], Oyetola Ogunkunle [3,*], Opeyeolu Timothy Laseinde [3], Ademola Oyejide Adebayo [1], Adeola Ibrahim Abdulkareem [1], Ghassan Fadhil Smaisim [4,5] and I.M.R. Fattah [6,*]

[1] Department of Agricultural Engineering, Ladoke Akintola University of Technology, Ogbomoso 210214, Nigeria
[2] Department of Chemical Engineering, Ladoke Akintola University of Technology, Ogbomoso 210214, Nigeria
[3] Department of Mechanical and Industrial Engineering Technology, University of Johannesburg, Johannesburg 2028, South Africa
[4] Department of Mechanical Engineering, Faculty of Engineering, University of Kufa, Najaf 54001, Iraq
[5] Nanotechnology and Advanced Materials Research Unit (NAMRU), Faculty of Engineering, University of Kufa, Najaf 54001, Iraq
[6] Centre for Technology in Water and Wastewater (CTWW), Faculty of Engineering and IT, University of Technology Sydney, Ultimo, NSW 2007, Australia
* Correspondence: ctoloyede@lautech.edu.ng (C.T.O.); oogunkunle@uj.ac.za (O.O.); islammdrizwanul.fattah@uts.edu.au (I.M.R.F.)

Abstract: The use of biobased heterogeneous catalysts made from agricultural waste for producing biodiesel has gained attention for its potential to create a sustainable and low-cost process. The blending of two or more biomass residues to create more viable biobased catalysts is still in its early stages. In this study, a Biobased Composite Heterogeneous Catalyst (CHC) was made by blending the shells of periwinkle (PWS), melon seed-husk (MSH), and locust bean pod-husk (LBP) at a mixing ratio of 67:17:17 using Simplex Lattice Design Mixture, that was then calcined for 4 h at 800 °C. The chemical, structural, and morphological components of the CHC were characterized via XRF, XRD, SEM-EDX, BET, TGA/DSC, and FTIR to assess its catalytic potential. The CHC was employed to synthesize biodiesel from palm kernel oil, and the process optimization was conducted using the Taguchi approach. The XRF analysis showed that the catalyst had 69.049 of Calcium (Ca) and 9.472 of potassium (K) in their elemental and oxide states as 61.592% calcium oxide and 7.919% potassium oxide. This was also supported by the EDX result, that showed an appreciable value of 58.00% of Ca and 2.30% of magnesium, that perhaps provided the active site in the transesterification reaction to synthesize biodiesel. The morphological and physisorption isotherms via SEM and BET showed mesoporous structures in the CHC that were made up of nanoparticles. A high maximum biodiesel yield of 90.207 wt.% was attained under the optimized process conditions. The catalyst could be reused for up to four cycles, and the biodiesel produced met both ASTM D6751 and EN 14214 standards for biodiesel. This study demonstrates that blending PWS, MSH, and LBP waste materials can produce high-quality biodiesel without the need for additional catalysts.

Keywords: agricultural residues; heterogeneous catalyst; characterization; biodiesel; optimization

Citation: Oloyede, C.T.; Jekayinfa, S.O.; Alade, A.O.; Ogunkunle, O.; Laseinde, O.T.; Adebayo, A.O.; Abdulkareem, A.I.; Smaisim, G.F.; Fattah, I.M.R. Synthesis of Biobased Composite Heterogeneous Catalyst for Biodiesel Production Using Simplex Lattice Design Mixture: Optimization Process by Taguchi Method. *Energies* **2023**, *16*, 2197. https://doi.org/10.3390/en16052197

Academic Editor: Domenico Laforgia

Received: 20 January 2023
Revised: 21 February 2023
Accepted: 22 February 2023
Published: 24 February 2023

1. Introduction

One of the hottest topics in the world right now is creating a sustainable environment devoid of the harmful gases that internal combustion engines (ICE) release into the atmosphere. Using green and renewable fuels produced from biological materials makes it possible to create a sustainable green environment. Researchers around the world are

actively looking for alternative biofuels that are both safe for the environment and renewable [1]. This is due to the fact that petrol-diesel fuels derived from hydrocarbon deposits are nonrenewable, contribute to greenhouse gases, and are gradually depleting [2]. Similarly, sustainable and renewable energy sources have become critical for any developing economy seeking to balance energy security and environmental conservation. As a result, fossil-derived fuels must be completely or partially replaced [3]. Biodiesel is one of the most commonly used biofuels to achieve these requirements [4,5]. It is similar to regular diesel and is produced from animal fats, vegetable oils, or used cooking oil. Biodiesel could replace fossil diesel fuel as it is biodegradable and has the ability to be used in practically all diesel engines and vehicles [6,7]. Biodiesel is typically produced through a catalyzed transesterification reaction. This reaction is a well-known chemical mechanism that involves the transformation of natural fats and oils to synthesize fatty acid ethyl ester (FAEE) or fatty acid methyl ester (FAME), as well as glycerol as a byproduct [8,9]. This reaction can be conducted using homogeneous, heterogeneous, or enzymatic catalysis [10,11].

Transesterification reactions for biodiesel production are typically accelerated using homogeneous or heterogeneous catalysis. Homogeneous catalysts have some advantages, such as low cost, fast reaction times, high catalytic activity, and suitable working conditions [12,13]. However, homogeneous catalysts also have limitations that hinder their widespread use in biodiesel synthesis. The catalyst usually absorbs moisture during storage [14]. Furthermore, purification methods necessitate multiple washes. These limitations make it challenging to eliminate sodium, potassium, and glycerol residues from biodiesel [14]. The heterogeneous catalyst is used to compensate for the negative effects of a homogeneous catalyst. Heterogeneous catalysts are environmentally friendly, easily separable from the reaction mixture, and renewable [10]. However, the biggest challenge to their use is the cost of synthetic heterogeneous catalysts, such as CaO, $Al(HSO_4)_3$, CaO-MoO_3, and lipases, that are expensive and difficult to produce in large quantities, making them less attractive for use in production processes [15–17].

The use of agricultural waste as a source of catalysts for biodiesel production is becoming increasingly popular due to its abundance, renewability, sustainability, and cost-effectiveness. Biobased or green catalysts are produced from natural sources containing alkalies or alkaline metals, such as sodium (Na), calcium (Ca), potassium (K), and magnesium (Mg) [10,13]. The development of biobased heterogeneous base catalysts from biomass agricultural residues necessitates several simple, low-energy processes. Several researchers have synthesized biodiesel using calcined biomass ash as a heterogeneous base catalyst. This is due to the presence of inorganic minerals in calcined biomass ash that act as active transesterification sites [18,19]. Several biobased heterogeneous base catalysts have been developed using calcined ash from various agricultural residues, including ostrich-eggshell [20], banana peels [21], rubber seed shells [22], ripe plantain-peel [23], *Brassica nigra* plant [24], walnut shell [25] and eggshell-moringa leaf [19,26]. These studies show that using heterogeneous catalysts in the production of biodiesel has resulted in significant success. Similarly, using agricultural residues to synthesize heterogeneous base catalysts would help to reduce environmental effects that endanger humans and animals [3,27]. It may also improve the viability of biodiesel production by removing barriers [19].

Recently, there has been increased interest in blending agricultural residues to provide an adequate amount of catalysts for biodiesel production. Olatundun et al. [28] used a mixture of raw cocoa pod husk and plantain peel to make a heterogeneous base catalyst for the transesterification of honne oil with methanol, yielding 98.98 wt.% biodiesel. Falowo et al. [3] recorded a maximum biodiesel yield of 98.45 wt.% using blended calcined kola-nut pod husk, cocoa pod husk, and plantain peel as heterogeneous catalysts for the transesterification of blended oil from hone, rubber, and neem seed oils. Following early research, periwinkle shells, melon husk, and locust bean husk have been identified as viable raw materials for industrial uses [10,29]. Oloyede et al. [10] have prepared biobased heterogeneous catalysts from these biogenic residues separately. Likewise, Okoye et al. [30] produced a heterogeneous catalyst using periwinkle shell. However, there appears to be

no information in the literature on the catalytic activity of the calcined ash obtained from the blend or mixture of these biogenic residues as a potential biobased composite heterogeneous catalyst for the transesterification reaction of oil. Similarly, the literature has not adequately reported the blending of calcined ash samples from agricultural residues using a Simplex Lattice Design Mixture (SLDM). Therefore, this study examined the development of an effective Composite Heterogenous Catalyst (CHC) from the blend of periwinkle shell, melon seed husk, and locust bean pod-husk using SLDM in Design Expert (13.0.1). The catalytic strength of the developed CHC was investigated using transesterification of palm kernel oil (PKO) with ethanol. The Taguchi orthogonal array method was used to model and optimize the transesterification factors.

2. Materials and Methods

2.1. Materials

The PKO used in this study was procured from a resident PKO production company in Ogbomoso, Nigeria. Melon seed and locust bean husks were sourced from Aroje (8°19′ N 4°26′ E), Ogbomoso, Nigeria, and periwinkle shells from Ondo state (6°21′ N 4°47′ E), Nigeria, because of their abundance in these regions. The ethanol (analytical grade of 99.9%) was bought from Savideb Laboratory Chemicals Enterprises, Osogbo, Nigeria.

2.2. Preparation of Catalyst Precursors

To remove dirt and obtain clean samples free of dust, the selected residues were rinsed with faucet water, followed by distilled water. The samples were sundried for three days before being oven-dried to a constant weight in a laboratory oven (Galenkamp 3456) at 373 K. Each residue was ground in an attrition mill and sieved to fine particle size using a mechanical shaker. Each sifted powdered sample was stored in sealed containers for further preparation.

2.3. Catalyst Preparation Using Simplex Lattice Design Mixture (SLDM)

Simplex Lattice Design is a boundary point design used to examine the blending of multiple components. This design is appropriate for 2 to 30 components. A simplex-lattice mixture design of degree m consists of m+1 points with equally spaced values ranging from 0 to 1. If m = 2, the possible fractions are 0, 1/2, and 1. For m = 3, the alternatives are 0, 1/3, 2/3, and 1. The points include the pure components as well as enough points between them to approximate an equation of degree m, and all of the design points are on the boundaries of the simplex [31]. In this study, a {3, 3} simplex lattice design that contains ten (10) blending coordinates (Figure 1) was used for the development of an effective CHC. The experimental region and the distribution of design run over the simplex region are shown in Figure 1.

The powdered samples from each residue (periwinkle shell, melon seed husk, and locust bean pod-husk) were blended at different ratios using the ratios obtained via SLDM in Design Expert (version 13.0.1). Table 1 shows the component levels fed into the SLDM and Table 2 shows the percentage blending ratio generated. A sample from each ratio was calcined in a muffle furnace at 1073 K for 240 min to remove organic materials and obtain fine ash [32]. The calcined ash obtained from each ratio was stored in airtight containers and in a desiccator for further investigation [3,19]. The calcined ash sample from each run (ratio) was used as a catalyst for the catalyzed transesterification of PKO with ethanol, with the goal of determining the ratio (run) with the highest biodiesel yield. The laboratory trial used to synthesize the biodiesel from each ratio was 7.0 wt.% CHC loading, 6:1 ethanol-to-PKO ratio, 65 °C and 120 min reaction temperature and time, respectively, under 700 rpm constant agitation speed. This speed (700 rpm) was chosen to improve the reactant during the transesterification process, allowing the reaction to start more quickly for maximum biodiesel yield. At the end of the catalyzed transesterification of PKO using catalyst from each ratio (run), the ratio that produced the catalyst that gave the highest biodiesel yield was selected as the appropriate ratio for the development of

CHC in this study. The CHC was then manufactured in large quantities and stored in an airtight container and a desiccator for further research. Further studies (characterization and transesterification) were carried out using the developed CHC. Hence, the further reports in this study are the results of the findings obtained on the catalytic activity of the developed CHC.

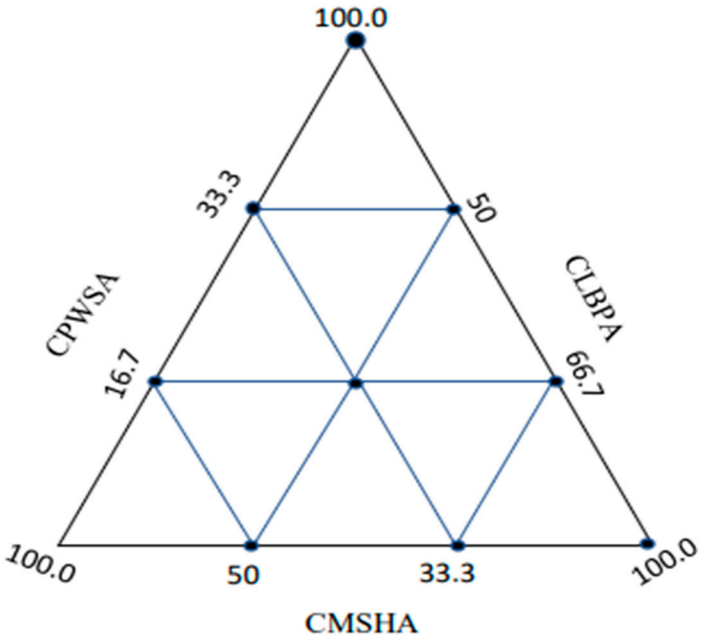

Figure 1. Design runs configuration for blending the samples using a {3,3} lattice mixture. Where PWSP is periwinkle shell powder, MSHP is melon seed husk powder, and LBPP is the locust bean pod-husk powder.

Table 1. Lattice design mixture for predicted mixing ratio.

Components		Levels	
Name	**Code**	**Low**	**High**
PWSP	A	0	100
MSHP	B	0	100
LBPP	C	0	100

Table 2. Simplex lattice design mixture ratio to develop the composite heterogeneous catalyst.

Run	PWSP (%)	MSHP (%)	LBPP (%)
1	0.0	100.0	0.0
2	33.3	33.3	33.3
3	100.0	0.0	0.0
4	0.0	50.0	50.0
5	50.0	50.0	0.0
6	50.0	0.0	50.0
7	0.0	0.0	100.0
8	16.7	66.7	16.7
9	66.7	16.7	16.7
10	16.7	16.7	66.7

2.4. Characterization of the Developed Biobased CHC

The specific chemical composition of the mineral phase of the developed biobased CHC was investigated via X-ray fluorescence spectroscopy (XRF) in an EPSILON 4 ED-XRF Analyzer (Malvern PanAnalytical, Almelo, the Netherlands). The crystal-like phases were

observed by utilizing an X-ray diffractometer (XRD) through a Rigaku-binary (Chicago, IL, USA). The sample was scanned continuously in locked coupled mode with Cu-K_2 radiation at a wavelength of 1.5444, a voltage of 45 kV, and a current of 40 mA. The rate of 5°/min in the 2–76° 2θ range was used to scan the sample [10]. The thermogravimetric or thermal stability (TGA/DSC) analysis of the catalyst was investigated using Perkin Elmer thermal analyzer (Diamond, IL, USA). The catalyst weight reduction was measured at the 30–1000 °C temperature range, with a heating rate of 10.00 °C/min and a steady supply of nitrogen gas (N_2). The catalyst functional groups were investigated via Fourier Transform Infrared (FTIR) spectra at a range of 400 to 4000 cm^{-1} by means of a Cary 630 FTIR spectrometer (Agilent Technologies, Santa Clara, CA, USA). The elemental composition was determined using Energy Dispersive X-ray (EDX) (JSM-7600F, Jeol Ltd., Tokyo, Japan), and a Gatan alto 2500 Cryo-system was used to produce the diffractograms. The CHC surface morphology was investigated using a scanning electron microscope (SEM) connected to an EDX spectrometer, while its textural analysis (surface area, pore volume, and pore particle size) was investigated using the Brunaeur-Emmet-Teller method (BET) on a Micrometrics Instrument (Micrometrics, ASAP-2021, V4.02H, Norcross, GA, USA). The basicity of the CHC was determined by dissolving 1.0 g of the CHC sample in 10 mL of distilled water, vigorously shaking, and leaving it to stand for 20 min [24]. The basicity of the aqueous solution was then verified using a digital pH meter (YK-P01, Amazon).

2.5. Transesterification Process of PKO Using the Selected CHC

The transesterification of PKO with ethanol to produce Palm Kernel Oil Ethyl Ester (PKOEE) was performed in a three-necked glass reactor with a capacity of 500 mL. The glass reactor was equipped with a glass reflux condenser on the neck to sustain the constancy of the ethanol-to-oil ratio, a thermometer for measuring the reaction temperature, a heating source controller for maintaining the reaction temperature, and a magnetic stirrer for continuous uniform blending of the mixture [33]. 100 mL ± 0.1 of PKO was poured inside the reactor and heated to the required temperature. The agitation speed was maintained at 700 rpm for continuous mixing. An exact quantity of catalyst (CHC) was measured and dissolved in a pre-measured quantity of ethanol (C_2H_5OH). Once the oil reached the required temperature, the prepared CHC-C_2H_5OH (catalyst-ethanol mixture) solution was gradually poured into the reactor. The completion of the pouring was taken as the beginning of the reaction. Once the predefined reaction time was reached, the glass reactor was taken out of the heating source, and the mixture was filtered through Whatman filter paper (100 microns) to separate the solid CHC [10]. The remaining reaction products were poured into a 500 mL separating funnel and allowed to stand for 1440 min (24 h) to ensure the complete settling of the products into two different layers. At the end of 24 h period, the glycerol layer was settled at the bottom of the separating funnel and removed via a drainage valve. The clear phase of PKOEE produced was obtained by washing the PKOEE with warm distilled water at 45 °C [23]. The biodiesel (PKOEE) was then placed on a heating plate at a temperature of 70 °C for 60 min to remove any traces of water [34] and then retained for further characterization. The percentage yield of PKOEE was calculated using the formula in Equation (1):

$$B_y\ (\%) = \frac{W_b}{W_{PKO}} \times 100 \quad (1)$$

where: B_y = PKOEE yield, W_b = mass of biodiesel produced, and W_{PKO} = mass of PKO used.

2.6. Research Experimental Design Using Taguchi Orthogonal Approach

Various factors, such as reaction rate or agitation, catalyst loading, reaction temperature, reaction time, and alcohol-to-oil ratio, affect biodiesel quality and yield. Additionally, the process parameters of catalyst loading, reaction temperature, alcohol-to-oil ratio, and reaction time are of particular importance [35]. It is difficult to predict the appropriate combination of process parameters in routine experiments for optimal biodiesel yield.

For example, for an optimization approach like that in this study, surface methodology combined with central composite design or Box–Behnken usually requires more experimentation to determine the optimal parametric conditions for each process [36]. Therefore, a well-organized design with less experimentation can eliminate cumbersome procedures for some combinations [37]. A new method of Design of Experiment (DOE) to consider the effects of different process parameters on the average and variance of performance characteristics that determine the proper functioning of a process has been developed by Dr. G. Taguchi.

This DOE method uses orthogonal arrays to optimize various parameters that affect the process and how they are changed. A special feature of this method is that it may not explore all possible combinations of process parameters involved in the optimization process, but the process can be reduced to a limited number of combinations, making data easier to analyze [37]. The required number of trials and their levels can be determined from an orthogonal array (OA). The number of variables and the different levels of each variable determines the choice of OA. In this work, the technique employed a factorial design of 3^4 via a Taguchi OA for the experimental conditions that were performed in the laboratory using the developed CHC. This was achieved using four appropriate process variables (factors) at three different levels, as shown in Table 3.

Table 3. Selected process parameters and their levels.

Parameters		Levels		
		1	**2**	**3**
A	Ethanol-to-PKO ratio	6:1	9:1	12:1
B	CHC loading, (wt.%)	3.0	5.0	7.0
C	Reaction temperature, (°C)	45	55	65
D	Reaction time (min)	40	80	120

A total number of arrays, L_9 (Table 4), was generated using the relation in Equation (2), as stated by Oladipo et al. [38].

$$N_e = 1 + (L - 1)F \quad (2)$$

where: N_e is the number of experimental runs, L is the number of levels, and F is the number of factors. The reaction condition chosen to predict biodiesel yield is the preferred value based on the operating conditions that significantly affect the biodiesel process.

Table 4. Taguchi L_9 orthogonal array for DOE with four parameters at three levels.

Run	Factors			
	A: EtOH: PKO	**B: CHC Loading (wt.%)**	**C: React. Temp. (°C)**	**D: React. Time (min.)**
1	9	5	65	40
2	9	3	55	120
3	6	7	65	120
4	12	7	55	40
5	9	7	45	80
6	6	3	45	40
7	6	5	55	80
8	12	5	45	120
9	12	3	65	80

2.7. Signal-to-Noise Ratio and Analysis of Variance (ANOVA)

Taguchi proposed using the loss function to compute the difference between the investigational and desired values of performance attributes. The loss function value was

then translated into a signal-to-noise ratio (SNR). SNRs are log functions of the predicted outcome that serve as the optimization problem's objective [37]. The SNR is then used to calculate the extent of the quality function's divergence from the expected value. Depending on the goal of the problem, the Taguchi approach employs three kinds of SNRs. The-Larger-the-Better (TLTB) method is used for maximizing problems, the the-Smaller-the-Better (TSTB) method for minimizing problems, and the the-Nominal-the-Better (TNTB) method for nominalizing problems. SNR may be computed from TLTB, TSTB, and TNTB models using Equations (3)–(5) [35].

$$\text{TLTB} - \text{SNR} = -log10\frac{1}{n}\left(\sum_{j=i}^{n}\frac{1}{y_j^2}\right) \tag{3}$$

$$\text{TSTB} - \text{SNR} = -log10\left(\sum_{j=i}^{n}\frac{y_j^2}{n}\right) \tag{4}$$

$$\text{TNTB} - \text{SNR} = log10\left(\overline{y}_i^2 / S_i^2\right) \tag{5}$$

But

$$y_i = \frac{1}{n}\left(\sum_{j=i}^{n} y_{i,j}\right) \tag{6}$$

$$s_i^2 = \frac{1}{n-1}\left(\sum_{j=1}^{n} y_{i,j-\overline{y}_i}\right) \tag{7}$$

where: y_i (Equation (6)) is response mean value, s_i^2 (Equation (7)) is the variance, i is the experimental number, j is the trial number, and n is the number of trials [35].

Since the aim in this study was to achieve a maximum biodiesel yield using the developed biobased CHC, the the-Larger-the-better SNR was adopted based on the nature of the variables. In order to enhance process efficiency, an SNR can be used to find the prime level of each parameter as well as its related set of ideal conditions. Unfortunately, the SNR is unable to identify the element that has a major influence on the output, as well as the extent to which each factor contributes to the output [35,36]. This can be understood by using ANOVA to estimate the statistical parameters. The impact factor for each individual variable on PKOEE yield provides information about its effect on the process and may be determined using the sum of squares of the individual components and the overall sum of squares of all input variables using Equation (8) according to Kumar et al. [35] and Oladipo and Betiku [38].

$$I_{f=}\frac{SS_y}{SS_T} \times 100 \tag{8}$$

where: I_f is the impact factor (%), SS_y is the summation of the square of the individual factors, SS_T is the overall sum of the square of all the process variables.

2.8. Physicochemical Properties of PKOEE Obtained Using the Developed CHC

The PKOEE obtained from the transesterification process using the developed CHC was characterized for its flash point, cloud point, kinematic viscosity, and density using ASTM D-93, ASTM D-2500, ASTM D445-19a, and ASTM D-1298, respectively. The calorific value and cetane number were calculated following the process detailed by Oloyede et al. [10]. The composition of fatty acid ethyl esters in PKOEE was determined using a SRI 910 Gas Chromatography (Buck Scientific Instruments, Norwalk, CT, USA) with 230 VAC ± 10%, a 1725 W power rating, and using Helium (He) as a carrier gas.

3. Results and Discussions

3.1. Selection of Effective CHC

The results obtained for each of the mixing ratios are shown in Table 5. As observed from Table 5, the ratio that gave the best PKOEE yield was during experimental run 9. The yield at this run was 86.68%, with a lattice mixing ratio of 66.7% CPWSA and 16.7% of both

CMSHA and CLBPA, respectively. The reason for this high PKOEE yield might be attributed to an increase in the catalyst active site in addition to the high composition of CaO in the mixture; this is justified by XRF, EDX, and XRD results. Oloyede et al. [10] reported the high composition of Ca for the CPWSA, CMSHA, and CLBPA and identified the active catalyst phases, such as CaO, K_2O, MgO, and other mixed metal oxides, might have contributed to the better yield during run 9. When the yields during run 3 (84.38%) and run 9 (86.68%) are compared, the difference between the values obtained was 2.30%. But, supposing the PKOEE was to be produced in metric tons industrially, the catalyst used during run 9 would be preferable for the transesterification reaction because a 2.30% difference becomes a major consideration for commercial production, even though it appears minor. Thus, the catalyst (CHC) during run 9 was characterized and subsequently used for the transesterification of PKO using the experimental design in Table 4. The PKOEE produced using this catalyst was analyzed for its physicochemical analysis and fatty acid compositions.

Table 5. Biodiesel yield and selection of effective composite heterogeneous catalyst.

Run	CPWSA (%)	CMSHA (%)	CLBPA (%)	Biodiesel Yield (%)
1	0.0	100.0	0.0	34.63
2	33.3	33.3	33.3	60.52
3	100.0	0.0	0.0	84.38
4	0.0	50.0	50.0	55.72
5	50.0	50.0	0.0	72.23
6	50.0	0.0	50.0	71.51
7	0.0	0.0	100.0	40.54
8	16.7	66.7	16.7	60.39
9	66.7	16.7	16.7	86.68
10	16.7	16.7	66.7	52.41

Note: CPWSA is Calcined Periwinkle Shell Ash, CMSHA is Calcined Melon Seed Husk Ash, and CLBPA is Calcined Locust Bean Pod Husk.

3.2. XRF Analysis of the Selected CHC

The XRF analysis was carried out on the developed biobased CHC to determine its chemical compositions. The results obtained for both the elemental and oxide composition of CHC are summarized in Table 6. The major components of the catalyst (CHC) were found to contain the elements and oxides of calcium (Ca), potassium (K), and silicon (Si). Other elements that formed the catalyst's chemical composition, present as trace elements, were iron (Fe), aluminum (Al), phosphorous (P), tin (Sn), and manganese (Mn). The oxides of Ca and K have been identified as the major components for catalytic activation [39]. The EDX and XRD results also confirmed this. Pathak et al. [39] observed similar metallic oxides for catalysts derived from *Musa acuminata* peel, but with K as the major element in that case. The oxides of Ca and K have been known to be strong bases that are primarily responsible for the catalyst's high basic nature in the transesterification reaction to produce biodiesel.

Table 6. XRF analysis of the selected CHC both elemental and oxide state.

S/N	Oxide	Result (%)	Element	Result (%)
1	CaO	61.592	Ca	69.472
2	SiO_2	14.198	K	9.472
3	K_2O	7.919	Si	8.375
4	P_2O_5	5.630	Fe	3.624
5	Fe_2O_3	2.983	P	3.204
6	Al_2O_3	2.729	Al	1.791
7	SO_3	1.509	S	0.805
8	TiO_2	0.405	Ti	0.418
9	Cl	0.236	Cl	0.324
10	Ag_2O	0.149	Ag	0.240
11			Mn	0.144

3.3. XRD Analysis of the Selected CHC

The related XRD diffractogram in Figure 2 describes the crystalline structure of the CHC. The presence of crystalline phases is indicated by the presence of multiple peaks in the diffraction peak centered at 2θ. The thermal decomposition via calcination triggered the chemicals in the CHC to decompose into CaO, $(Ca_{0.9}Mg_{0.1})CO_3$ (calcite-magnesium bearing), and SiO_2. The XRD spectrum revealed that the phases were dominated by $(Ca_{0.9}Mg_{0.1})CO_3$ and CaO compounds. The observation is consistent with the elemental composition determined by the EDX and XRF analyses, indicating that Ca is the most abundant element in the CHC. Furthermore, these findings are consistent with previous research on the catalysts derived from the calcined periwinkle shell, melon seed husk, and locust bean pod-husk that were blended in this study to synthesize the Composite Heterogeneous Catalyst. Suryaputra et al. [15] reported similar phases of CaO and calcite in Capiz shell calcined at 900 °C. However, KCl and $K_2Ca(CO_3)$ are the main phases in the calcined blended cocoa pod shell, plantain peel, and kola nut husk ashes-derived heterogeneous catalyst stated by Falowo et al. [3]. The existence of calcite phases in CHC shows that the sample could require calcination at higher temperatures (above 800 °C) for complete thermal decomposition of calcite.

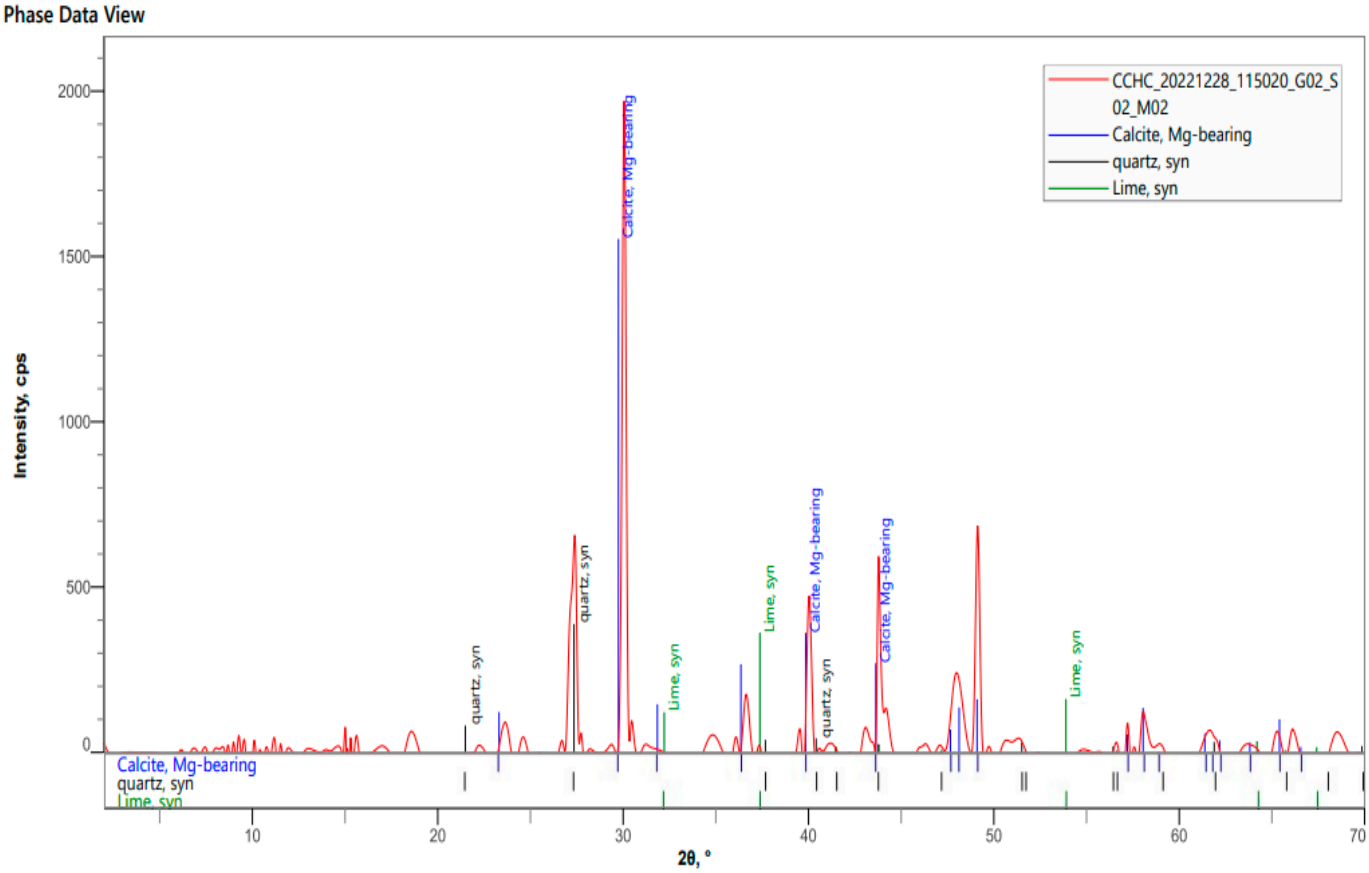

Figure 2. XRD diffractogram of selected CHC calcined at 800 °C.

3.4. TGA/DSC Analysis of the Selcted CHC

Figure 3A,B (replotted graphs) depict the TGA/DSC thermograms of the biobased composite heterogeneous catalyst. These figures indicate the percentage weight loss in relation to time and temperature, respectively. The weight of the catalyst sample used was 8.338 milligrams. The initial weight reduction was observed at about 370.21–626.3 K. This can be attributed to moisture evolution and the formation of Carbon (IV) oxide (CO_2) in the temperature range [40]. The weight of the CHC was further reduced due to the oxidation of carbonic material in the catalyst and the release of CO_2 from calcium carbonate, $CaCO_3$ [39].

The differential scanning calorimetry analysis, DSC, reveals that the phase transition of the thermal decomposition of CHC occurred at a time range between 0–20 min. The negative peak of the DSC indicates that the process was endothermic. This shows that the sample was exposed to more heat during calcination [41]. A similar outcome was reported for Mereterix's TGA by Nair et al. [42] and *Musa acuminata* peel by Pathak et al. [39].

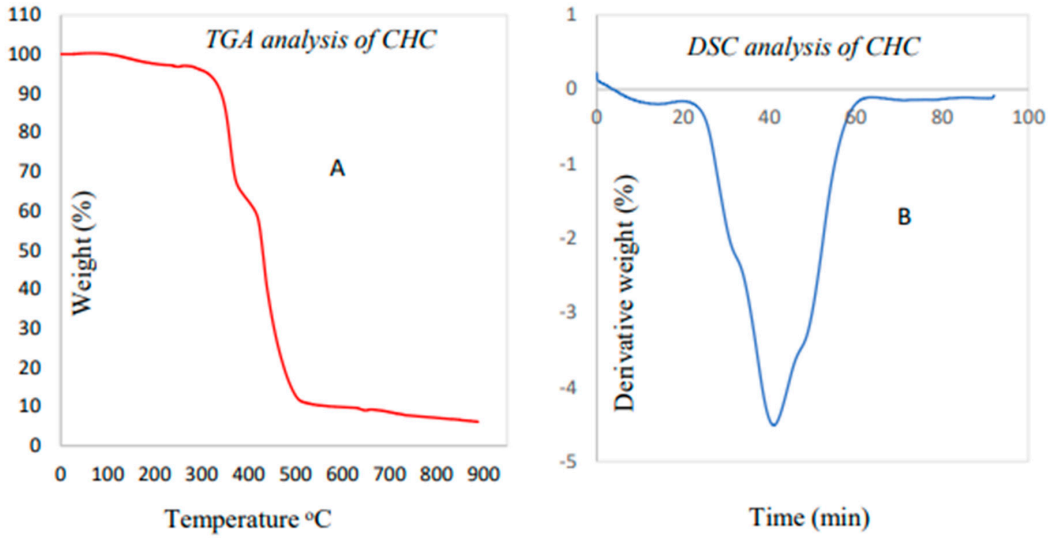

Figure 3. (**A**) TGA thermogram of CHC, (**B**) DSC thermogram of CHC.

3.5. FTIR Analysis of the Selected CHC

The FTIR pattern for the catalyst sample is shown in Figure 4. The characteristic absorption peaks of CHC are observed by IR spectra [10]. The major peaks of 1397.8 and 1036.2 cm^{-1} are associated with the asymmetrical bond of C=O and C-O groups in CO_3^{2-}. This may be due to the absorption CO_2 onto the surface of the metal oxide, thus suggesting the presence of the oxides of Ca, Mg, or K in the catalyst [10]. The absorption peaks at 872.2 and 711.9 cm^{-1} at the fingerprint region, which are attributed to out-of-plane bend vibration modes, may be due to the presence of -SiO_2 isolated vibration in Ca_3Al_2Si from interaction with Al^{3+} and Ca^{2+}. Similar interactions have been detected by Betiku et al. [6] and Oloyede et al. [10] for heterogeneous catalysts derived from kola nut pod husk and periwinkle shell, respectively. The FTIR results agreed with the XRF, EDX, and XRD data.

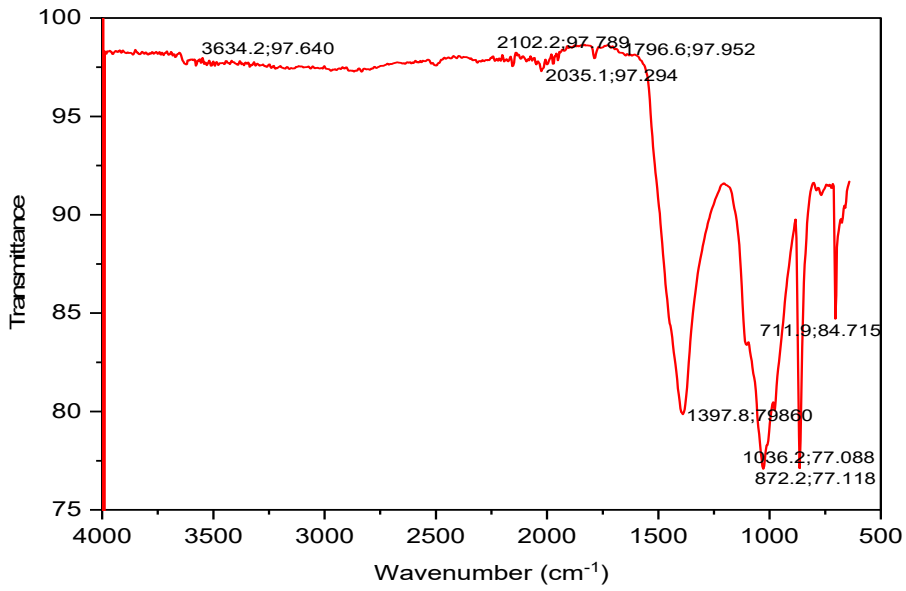

Figure 4. The FTIR spectral of the selected CHC.

3.6. EDX Analysis of the Selected CHC

The EDX spectra of the elemental composition of CHC analyzed via EDX are shown in Figure 5. It was observed that Ca had the highest mass fraction (58.0%), thus corroborating the XRF result. Magnesium (Mg) and sodium (Na) were present as trace elements, having a mass fraction of 2.3% and 1.1%, respectively. However, Mg and Na could not be detected by the XRF. This could be a result of the function of the machine. The EDX results of CHC agreed with the EDS result of $CPWSA_{800}$, $CMSHA_{800}$, and $CLBPA_{800}$ catalysts stated by Oloyede et al. [10]. The result also agreed with the XRD analysis of each of the catalysts, showing an appreciable scoring of the oxide of the alkaline metal present, as reported by Oloyede et al. [10]. A similar result was reported for the EDX and XRD results obtained for the cocoa pod husk-plantain peel blend by Olatundun et al. [28].

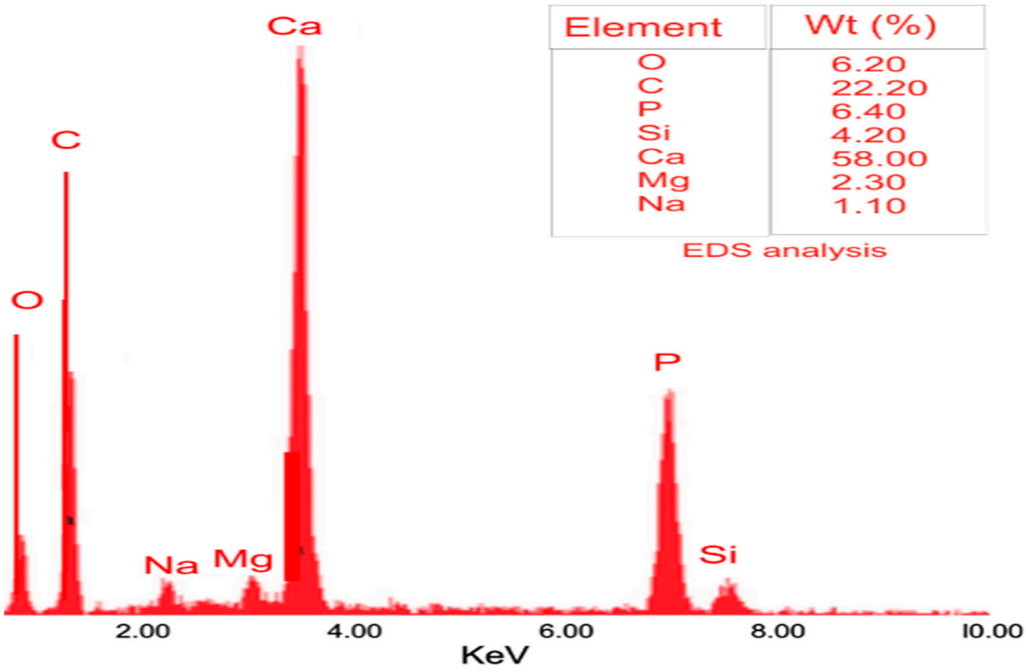

Figure 5. EDX elemental composition of the selected CHC.

3.7. SEM Analysis of the Selected CHC

The SEM image of the CHC was viewed at three resolutions (8000, 9000 and 10,000) and the result is shown in Figure 6. The images show the agglomeration of non-uniform particles, clusters of various shapes and sizes, and layered spongy fibrous microstructures that occur during calcination and are revealed in the three resolutions. However, the image at a resolution of 8000 showed a spongier microporous morphology. The bright particles seen in the SEM images might be due to the catalyst's oxygen-containing substances and may be metal oxides. Aleman-Ramirez et al. [18] also observed an agglomeration with a microporous morphology for a moringa leaves ash catalyst calcined at 500 °C. Similarly, Nath et al. [24] detailed that the SEM character of a catalyst prepared from the *Brassica nigra* plant for transesterification of soybean oil indicated the agglomeration of particles and layered spongy stringy microstructures [43].

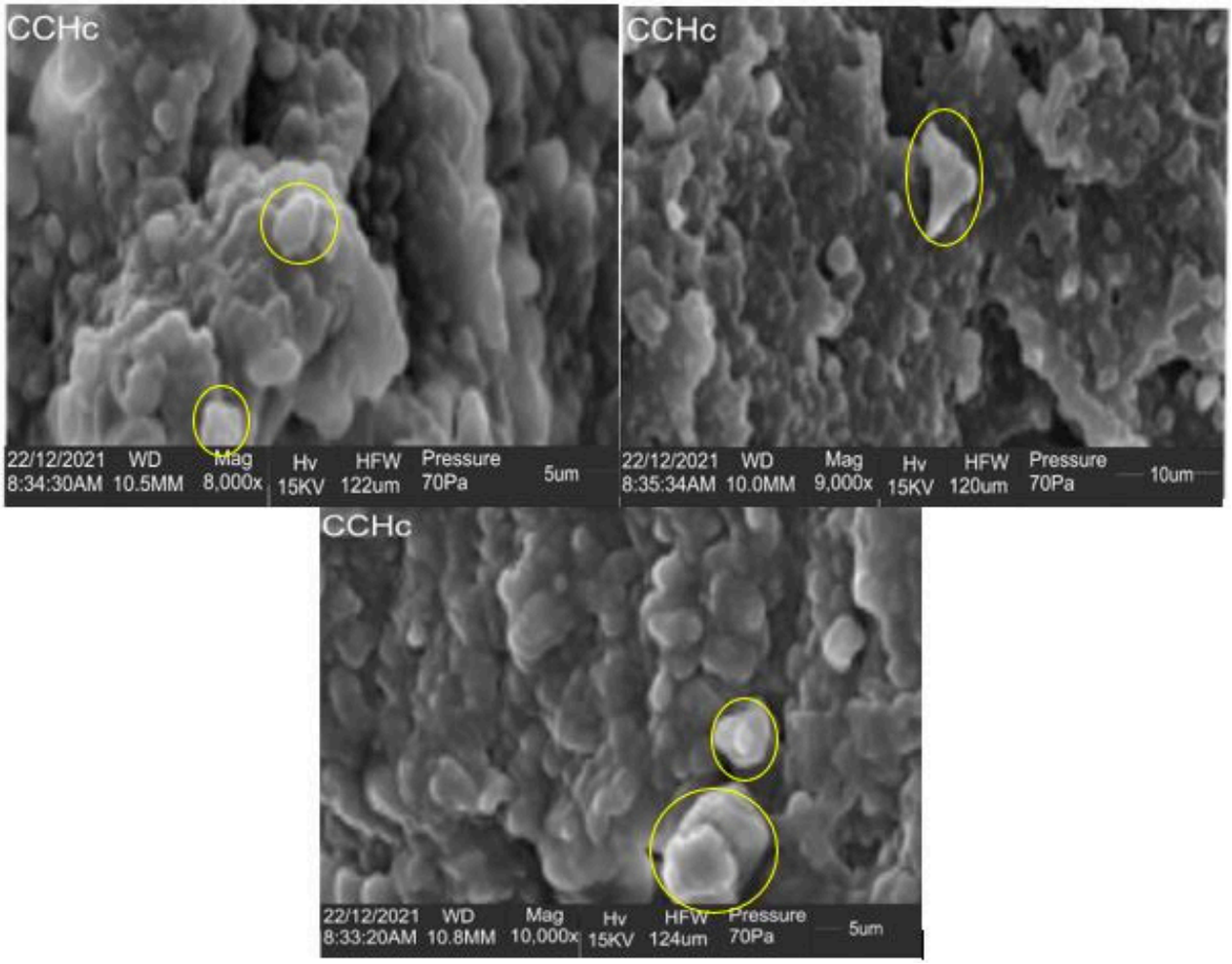

Figure 6. SEM image of CHC at different resolutions.

3.8. N_2 Physical Adsorption of the Selected CHC

How active a catalyst is will be significantly impacted by the surface area and pore size of all sorts of heterogeneous solid catalysts, in addition to mineral content [44]. The surface area, pore volume, and pore size of the CHC were examined by the BET technique and were found to be 215. 5 $\pm$ 3.3 m^2g^{-1}, 0.4903 cm^3g^{-1}, and 2.022 nm (20.220 Å), respectively. This indicates the presence of a mesopore. The large surface area of the catalyst indicates that the ash sample could have good catalytic activity. According to Betiku et al. [6], a catalyst with a large surface area facilitates increased interaction between reactants and catalyst active sites. Gohain et al. [45] reported similar values of 78.681 m^2g^{-1}, 0.349 ccg^{-1}, and 1.6074 nm for surface area, pore volume, and pore radius, respectively, for the calcined *Carica papaya* stem (CCPS). However, the surface area reported for the CCPS is lower than the obtained value for the CHC. The N_2 adsorption-desorption isotherms and pore size distribution for the CHC catalyst are shown in Figure 7a,b. The N_2 adsorption-desorption primarily resembles a type IV isotherm with an adsorption hysteresis loop of type H_3 that resembles a capillary condensation that occurs in a mesopores, thus indicating that CHC is a mesoporous nanomaterial [28]. The distribution of the CHC pore size was between 1.0 to 100.0 nm (10 to 1000 Å) (Figure 7b).

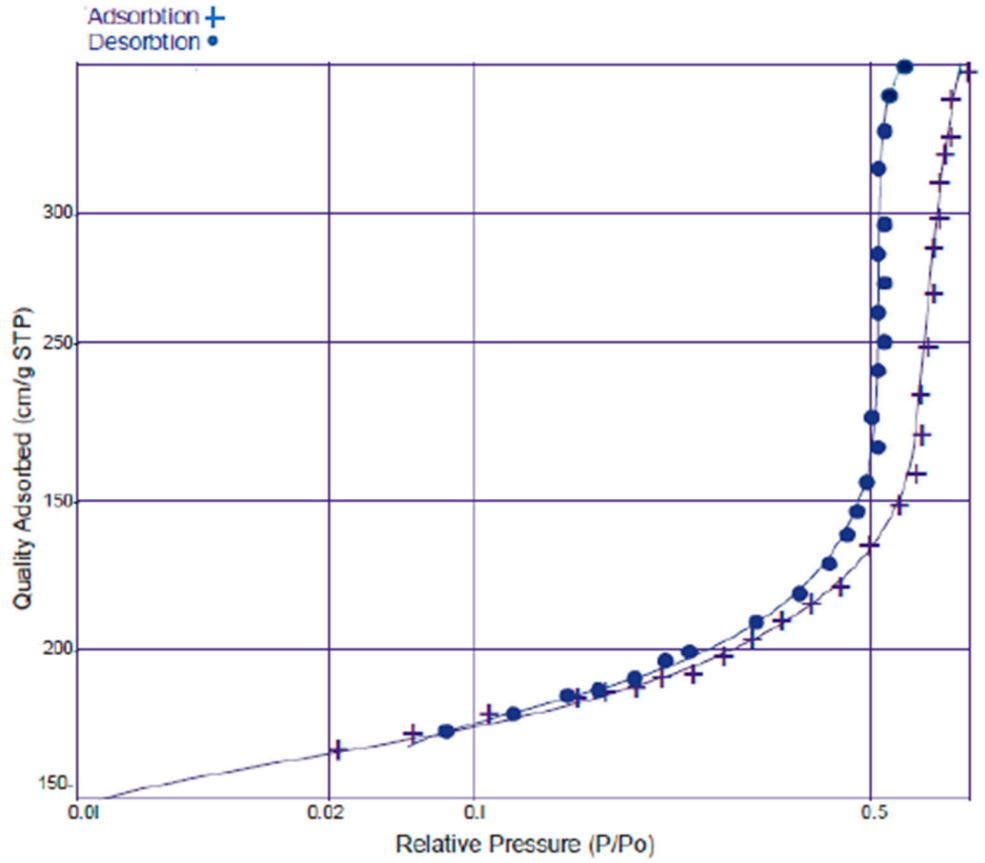

(**a**)

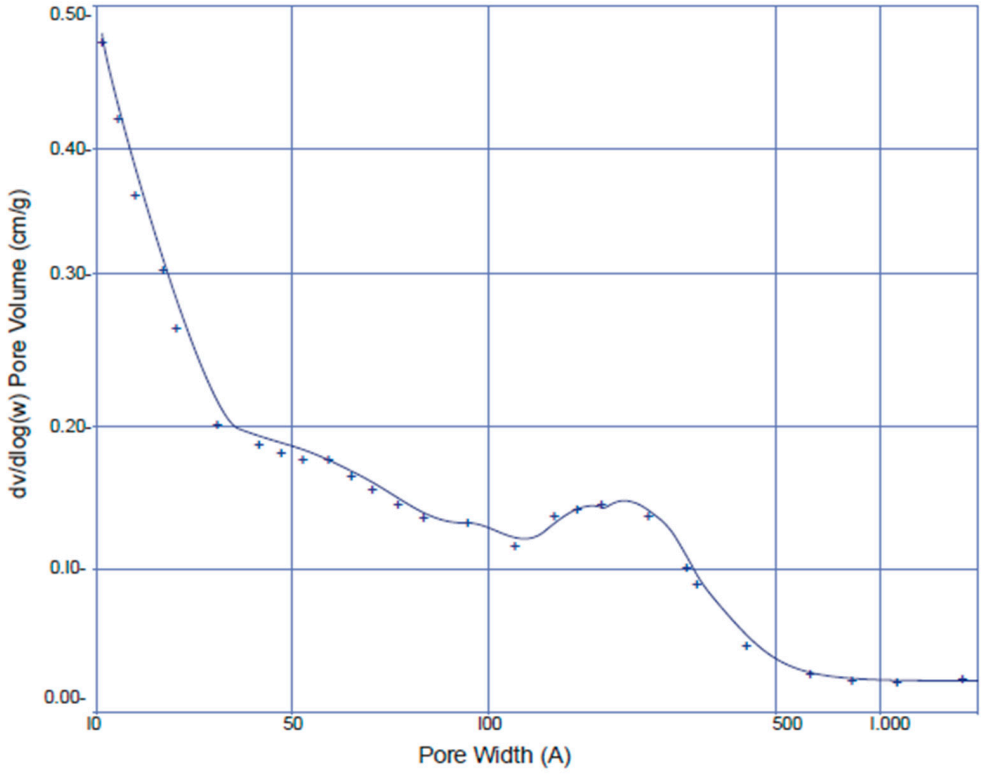

(**b**)

Figure 7. (**a**): N_2 adsorption-desorption isotherm of the selected CHC; (**b**): Pore size distribution of the selected CHC.

3.9. Basicity of the Selected CHC

Knowing the basicity of a catalyst is important in understanding the behavior of such a catalyst during a catalyzed transesterification reaction [18]. The CHC pH mean value was 11.08, indicating that the catalyst has a high basicity. According to the EDX and XRF analyses of the sample, this behavior could be attributed to the greater mass fraction of alkaline metals contained in the catalyst. This must have influenced the yield of PKOEE during the transesterification reaction. When Nath et al. [24] investigated the basicity of catalyst production from the *Brassica nigra* plant, they found a pH value of 11.91 when 1.0 g of the catalyst sample was liquified in 5 mL of water. Showing that the selected CHC possesses good basicity.

4. Catalytic Performance of the Selected CHC via Transesterification of PKO

Catalyzed transesterification of PKO was used to test the catalytic behavior of the selected CHC. Table 7 displays the PKOEE results obtained using this catalyst and includes the design matrix and experimental PKOEE yields. The maximum and minimum PKOEE yields obtained were 86.72 and 71.31% during run 3 and run 2, respectively. This substantial PKOEE output during run 3 could be attributed to the moderate reaction variables, which were sufficient to cause PKOEE formation [46]. Falowo et al. [3] detailed a similar result in the transesterification of blended hone-rubber-neem oils using a heterogeneous catalyst developed from a blend of calcined cocoa pod husk, plantain peel, and kolanut shell and obtained a biodiesel yield of 98.45%. Also, Aleman-Ramirez et al. [19] detailed a biodiesel yield of 94.3% for soybean oil using a composite heterogenous catalyst produced from the mixture of eggshell and moringa leaf. However, the obtained PKOEE yield in this study is lower compared with that of Falowo et al. [3] and Aleman-Ramirez et al. [19]. This may be attributed to the incomplete thermal decomposition of CHC, which indicates the presence of $CaCO_3$ in the CHC via XRD [10].

Table 7. PKOEE yield using CHC developed using SLDM.

Run	Factors				Response
	A: EtOH: PKO	**B: Catalyst Loading**	**C: React. Temp.**	**D: React. Time**	**Biodiesel Yield**
		(wt.%)	**(°C)**	**(min.)**	**%**
1	9	5	65	40	81.56
2	9	3	55	120	71.31
3	6	7	65	120	86.72
4	12	7	55	40	80.50
5	9	7	45	80	81.60
6	6	3	45	40	77.60
7	6	5	55	80	73.61
8	12	5	45	120	84.10
9	12	3	65	80	85.20

4.1. Physicochemical Studies of PKOEE Produced Using the Selected CHC

The physical and chemical properties of PKOEE synthesized using the selected CHC are detailed in Table 8. Since all fatty acid alkyl esters must meet the quality standards defined by ASTM D6751 or EN142144 to meet global acceptance, the quality of the PKOEE produced was compared against these two standards. The PKOEE sample produced had a kinematic viscosity of 4.74 mm^2/s. Odude et al. [47] reported a kinematic viscosity of 35.4 mm^2/s for palm kernel oil in a recent study. Hence, the 4.74 mm^2/s obtained for the PKOEE in this study showed a reduction of 86.6% in the viscosity of PKOEE using CHC. The value obtained is close to the 4.64 mm^2/s reported by Akhabue et al. [48] for a PKO biodiesel using CaO derived from chicken eggshell as catalyst. This implies that the biodiesel produced in this study has the tendency to run smoothly in CIE and may have good fuel atomization [4]. The specific gravity of the obtained PKOEE is 0.832. This value

satisfies the limits set by ASTM-D1298 (0.860–0.90). This shows that the specific gravity of PKOEE may be useful to grade its energy content, estimate its performance in CIE, and be used in connection with fuel storage and transportation [46]. Aladetuyi et al. [49] reported 0.8624 for the density of a PKO biodiesel produced using cocoa pod-husk ash (CPA) as the catalyst. The low-temperature flow properties (flash, cloud, and pour point) of the PKOEE are 214, +5, and −3.0 °C, respectively. These values compared favorably with the reported values for the low-temperature flow properties studied by Akhabue and Ogogo [50] and Olutoye et al. [51]. The PKOEE has a cetane number and calorific value of 72.68 and 8.96 MJ kg^{-1}, respectively. Oladipo and Betiku et al. [38] obtained values of 59.54 and 40.32 MJ kg^{-1}, respectively, for the biodiesel produced from rubber seed oil (*H. brasiliensis* oil) using kola nut pod husk ash as the catalyst. The calorific value of PKOEE obtained in this study is significantly lower than the one reported for the *Havea brasiliensis* oil methyl ester (HBOME). This could be as a result of the difference in the oil sample used. The higher the cetane number, the better the ignition quality [4]. Hence, there is an indication that the PKOEE produced using CHC may produce a better ignition quality when used in CIE.

Table 8. Physicochemical analysis of PKOEE produced using the developed CHC.

Fuel Properties	Unit		Test Method	ASTM-D6751 Biodiesel Standard	EN 14214
Kinematic viscosity at (40 °C)	mm^2/s	4.5	D455/EN3104	1.9–6.0	3.5–5.0
Specific gravity		0.872	D4052	0.86–0.9	0.85
Flash point	°C	218	D93/EN3679	93–130	120 min
Cloud point	°C	+7	D2500/EN23015	NR	NR
Iodine value	g I_2 $100g^{-1}$	72.1	D664/EN14111	NR	120 max
Saponification Value	Mg KOH	120.4	NR	NR	NR
Cetane number		30.53	D613/EN5165	47 min	51 min
Calorific value	MJ kg^{-1}	8.54	NR	NR	NR
Pour point	°C	+4.0	D97/EN3016	NR	NR

4.2. ANOVA of Transesterification Process of PKO Using the Selected CHC

The PKO was transesterified using a set of parametric settings obtained from the experimental matrix designed by Taguchi L9 orthogonal array. The analysis of variance (ANOVA) for statistically validated models for the PKOEE yield response is summarized in Table 9. The three instrumental variables (ethanol-to-PKO ratio, CHC loading, and reaction temperature) are significant ($p < 0.05$) according to Table 9. The F and *p*-values were calculated to determine the significance of the model and each process parameter. Its significance is confirmed by the high model F-value (65.69) and low *p*-value (0.0151). The F-value indicates a substantial model, and there is only a 1.51% probability that such a model could exist due to noise. Model terms with *p*-values less than 0.05 are considered significant. Factors A, B, and C are significant model terms in this scenario, with *p*-values of 0.0247, 0.0285, and 0.008, respectively. As a result, the reaction temperature was discovered to be the most important variable in the model, with the greatest F-number (134.32) and the lowest *p*-value (0.008). A similar observation was reported for the factors examined for the optimization of biodiesel produced from rubber seed oil by Oladipo and Betiku [38] using the Taguchi L9 technique. Factors B (catalyst concentration), C (reaction temperature), and D (reaction time) were reported to be significant model factors with *p*-values of 0.106, 0.0116, and 0.0069, respectively. This means that the *p*-values obtained for the variables in this study compared favorably to the values published in earlier similar studies.

Table 9. Test of significance for the regression model and process variables.

ANOVA						
Source	**Sum of Squares**	**df**	**M-Square**	**F-Value**	***p*-Value**	
Model	214.38	6	35.73	65.69	0.0151	Significant
A-EtOH: PKO	43.01	2	21.51	39.54	0.0247	
B-Catalyst loading	37.05	2	18.52	34.06	0.0285	
C-Reaction temp.	134.32	2	67.16	123.48	0.0080	
Residual	1.09	2	0.5439			
Corrected Total SS	215.47	8				

4.3. Determination of Variable Impact Factor of the Transesterification Process

Individual parameter importance is proven by determining the impact factor of each parameter in the process. Figure 8 depicts the effect factor of each process variable as computed by Equation (8). The results confirmed that the reaction temperature has the largest impact factor of 62.34%, which substantially affects the process, followed by the ethanol-to-oil ratio and catalyst loading, both of which have impact factors of 19.96% and 17.19%, respectively. The values show that the ANOVA results match well with the impact factor results and that reaction temperature significantly affects biodiesel yield. Saravanakumar et al. [52] found a comparable result using Taguchi L9 for the optimization of biodiesel production from *Pungamia* oil, where stirrer speed was the most important parameter in the transesterification process. Likewise, the reaction temperature was reported by Olatundun et al. [28] as the most significant parameter with an impact factor of 60.93% using the Taguchi L9 approach. At the same time, reaction time and catalyst concentration were detailed as the most significant variable with an impact factor of 60.41 and 67.34% by Oladipo and Betiku [38] and Kumar et al. [35], respectively.

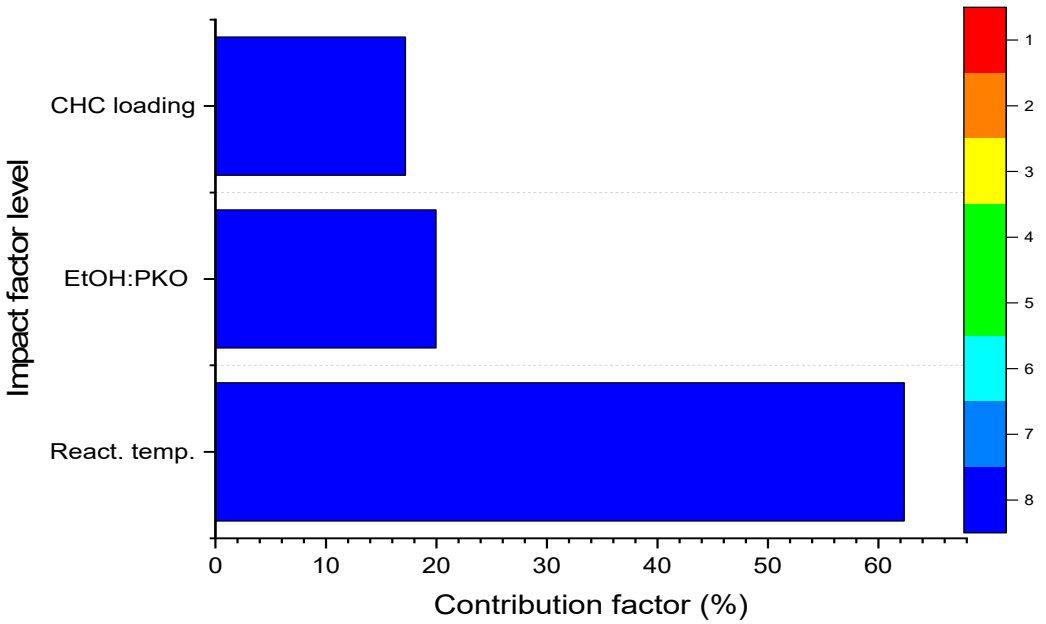

Figure 8. Impact level of input variables on PKOEE produced using the selected CHC.

4.4. Mathematical Model Equation for the Transesterification Process

An ANOVA study was used to analyze both the model and individual parameters. The significant parameters influencing the process parameters were determined. For this current investigation of PKO transesterification using the developed CHC, the regression analysis takes into account the significant parameters while discarding the inconsequential ones [37]. In the mathematical model equation (Equation (9)) for predicting PKOEE yield,

the coefficients of each significant parameter determined with a 95% ($p < 0.05$) confidence level were considered.

$$(B_y wt.\%) = 80.25 - 0.937A[1] - 2.08A[2] - 2.20B[1] - 0.490B[2] + 0.853C[1] - 5.10C[2] \quad (9)$$

where: B_y is the PKO biodiesel yield, $(wt.\%)$, A is the ethanol-to-PKO ratio, B is the CHC loading, $(wt.\%)$, C is the reaction temperature, (°C), and [1] and [2] are the levels of each factor. Based on the studies by Oladipo and Betiku [38] and Olatundun et al. [28], the methanol-to-oil ratio and reaction time, respectively, were excluded from the mathematical model because they were statistically insignificant ($p < 0.05$). The model's experimental and predicted values, which assess the model, are shown in Figure 9. The graph shows the correspondence between the two datasets. The approximation points are almost diagonal, thereby showing the accuracy of the model in explaining the process.

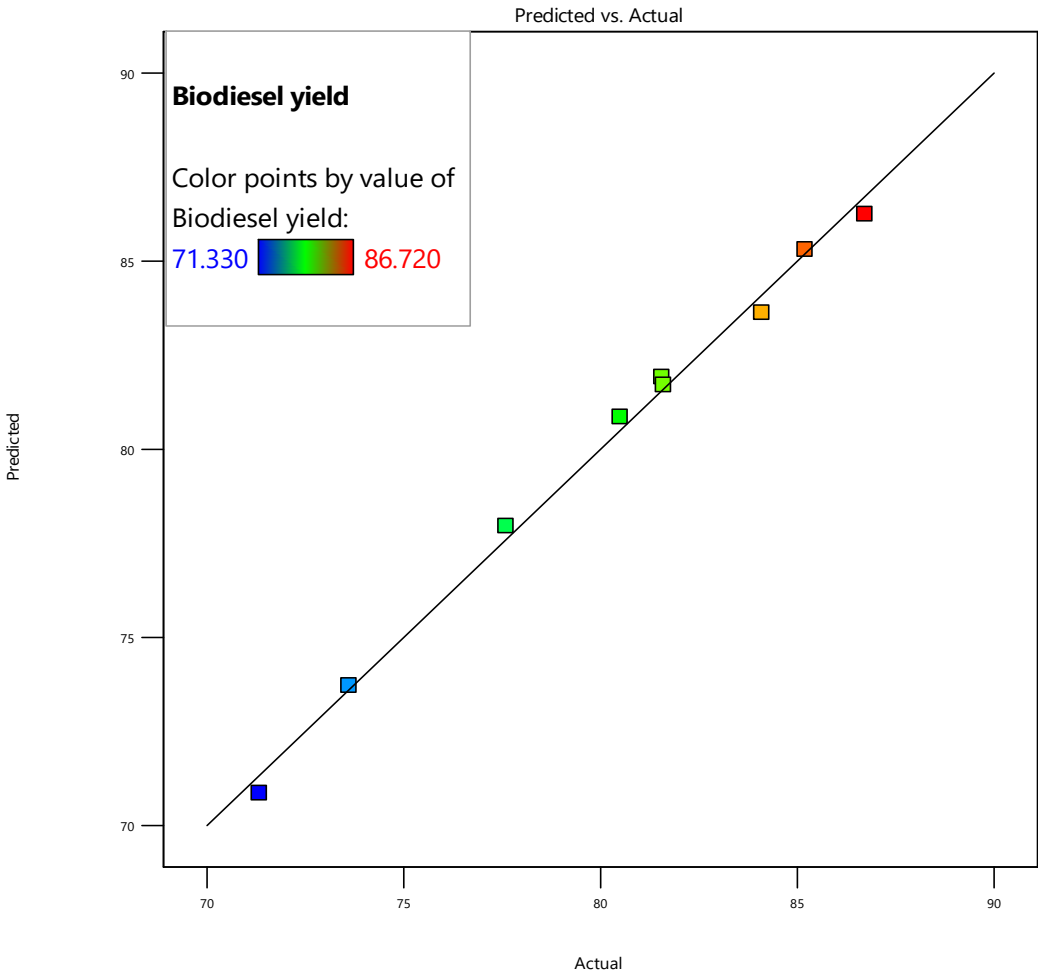

Figure 9. Plot of predicted value against experimental value of PKOEE (Biodiesel) yield.

The quality of the model fit and its statistical significance were evaluated. A high correlation coefficient (R^2) of 0.9950 for the model indicates that a good match exists between the experimental and predicted PKOEE (biodiesel) yield. This shows that 99.50% of the sample variation for the PKOEE yield is attributed to the independent variables, and just 0.5% of the total variation was not defined by the model [21]. The p-values less than 0.05 indicate that model terms are significant. The adjusted R^2 value of 0.9798, which was used to check the overestimation of the R^2, was sufficiently high to confirm the importance of the model. Also, the high value of 0.8978 obtained for the predicted R^2 is in reasonable agreement with the adjusted R^2 value. This helps the accuracy of the fitted model because the deviation (0.082) between the two is less than the maximum tolerance of 0.2 for the

deviation. The standard deviation, the mean of response, and the coefficient of variance (CV) of the model were 0.7375, 80.25, and 0.919%, respectively. Hence, the low standard deviation and CV of less than 10% means that the experimental and predicted values agreed [21].

4.5. Numerical Optimization for the Transesterification Process

The numerical optimization of the data obtained was conducted using the Design Expert Software (13). The highest desirability selected for the transesterification of PKO was 1.000. The highest limit for the PKOEE yield was set to "maximize", while the processing variables were all set within the range between the minimum and maximum values selected. The constraints for the numerical optimization process to produce PKOEE are computed in Table 10. After processing, solutions for 78 combinations were suggested by the software; solutions with a desirability level of less than 1.00 were rejected, leaving 9 solutions (Table 11). It was observed that the reaction conditions at numbers 1, 4, and 5 have an equal optimum PKOEE yield (90.207%) with the same reaction conditions but different reaction time levels. However, since the optimum biodiesel yield (90.207%) was predicted to be achieved at a minimum reaction time of 40 min when compared with other options, the reaction conditions at number 4 were selected.

Table 10. Constraints for the numerical optimization process to produce PKOEE using CHC.

Name	Unit	Goal	Lower Limit	Upper Limit
A: EtOH: PKO molar ratio		is in range	6	12
B: Catalyst loading	wt.%	is in range	3	7
C: Reaction temperature	°C	is in range	45	65
D: Reaction time	min.	is in range	40	120
Biodiesel yield	%	maximize	71.33	86.72

Table 11. Solutions for the combinations of numerical factor levels.

Number	EtOH:PKO	Catalyst Loading	Reaction Temp.	Reaction Time	Biodiesel Yield	Desirability	
1	12	7	65	120	90.207	1.000	
2	12	5	65	40	87.023	1.000	
3	12	7	45	80	86.813	1.000	
4	12	7	65	40	90.207	1.000	Selected
5	12	7	65	80	90.207	1.000	
6	12	7	45	40	86.813	1.000	
7	12	5	65	80	87.023	1.000	
8	12	5	65	120	87.023	1.000	
9	12	7	45	120	86.813	1.000	

4.6. Model Validation of the Optimization Process

Laboratory experiments were carefully conducted in three iterations using the optimum reaction conditions. An average PKOEE yield of 86.69% was observed (Table 12) using the selected CHC. The error difference between the optimum numerical value (90.207%) and the experimental value was 3.90%. This implies that the experimental value is somewhat consistent with the value predicted by the model. Therefore, this further demonstrates that the model is suitable for describing the PKO biodiesel conversion process. Dhawane et al. [53] observed a similar trend for biodiesel produced from waste cooking oil. An FFA conversion of 94.82% was reported at the optimum reaction condition time of 180 min, with a methanol-to-oil molar ratio 12:1, catalyst concentration of 5.0 wt.%, and reaction temperature of 60 °C. This revealed that the optimal reaction condition obtained in this study matched those previously reported in similar studies.

Table 12. The average yield of experimental results for the predicted optimal level.

	PKOEE Yield (%)	Desirability
Experiment 1	86.69	
Experiment 2	86.70	
Experiment 3	86.68	
Average	86.69	
Numerical optimization	90.21	1.000
% Difference	3.90	

4.7. Impact of Process Variables on Palm Kernel Oil Ester Yield

4.7.1. Impact of Ethanol-to-Oil Ratio on PKOEE Yield Using the Selected CHC

The effect of ethanol-to-oil ratio (6:1, 9:1, and 12:1) on the yield of PKOEE obtained at the optimum reaction condition of a 7.0 wt.% CHC loading, a 65 °C reaction temperature, and a reaction time of 120 min is displayed in Figure 10. It was observed that the PKOEE yield decreased faintly from 86.72 to 85.10% when the EtOH-to-PKO ratio increased from 6:1 to 9:1. This may be because there was less interaction between the catalyst and reactants. By increasing the EtOH-to-PKO ratio, the PKOEE yield was expected to increase. A significant increase of 90.2% was obtained as the EtOH-to- PKO ratio increased to 12:1. This may be due to th since transesterification is an equilibrium reaction and both forward and backward reactions can be catalyzed by the base. A reversible reaction may occur due to a high concentration of ethanol in the reaction forming diglyceride and triglyceride, thereby resulting in a high yield of PKOEE [28,39]. This agreed with the discoveries by Olatundun et al. [28], who reported a higher biodiesel yield of 98.98% at a methanol-to-oil ratio of 12:1 for the transesterification of *honne* oil using calcined cocoa pod husk-plantain peel blend as a catalyst. This revealed that this current result corresponds with the previously reported similar studies.

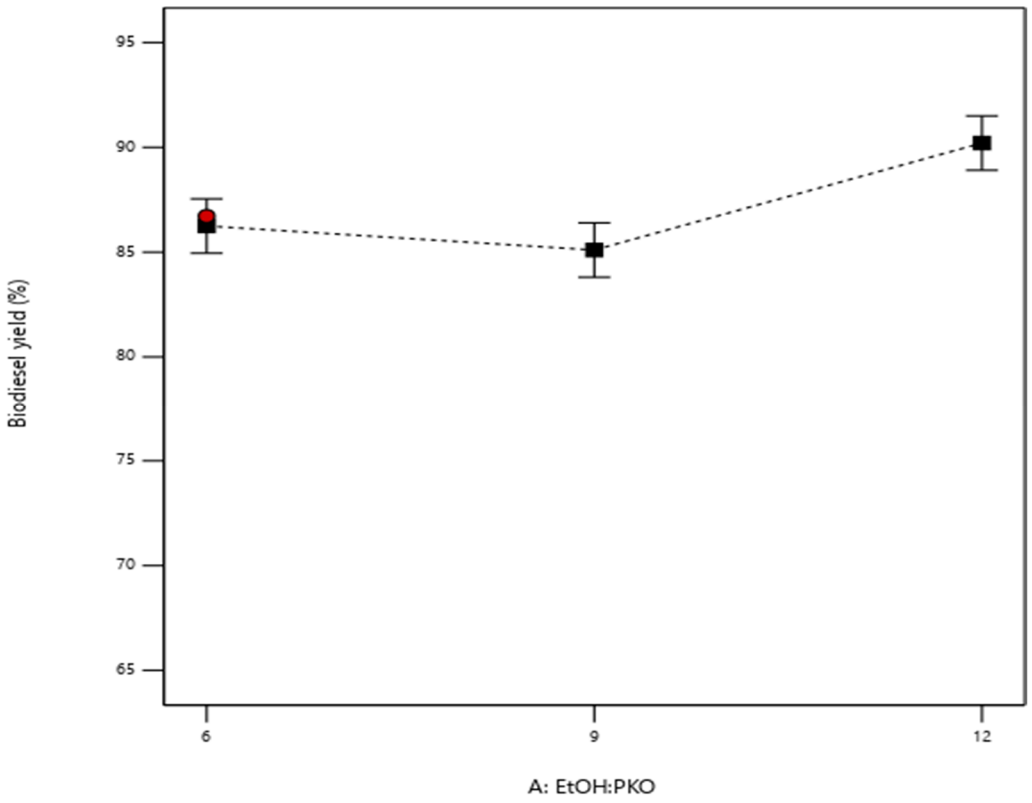

Figure 10. Impact of ethanol-to-oil ratio on PKOEE yield obtained using the selected CHC.

4.7.2. Impact of Catalyst Loading on PKOEE Yield Obtained Using the Selected CHC

The amount of catalyst in relation to the amount of oil influences the rate of transesterification [33]. To investigate the influence of catalyst loading on PKOEE yield, different catalyst amounts of 3.0, 5.0, and 7.0 wt% were used, while all other process variables remained constant (an ethanol-to-oil ratio of 6:1, reaction temperature of 65 °C, and reaction time of 120 min). Figure 11 depicts the effect of catalytic loading. The figure shows that, as catalyst loading increased from 3% to 7%, the yield of PKO biodiesel increased from 81.35% to 86.72%. The rise in PKOEE yield from low to high catalyst concentrations might be attributed to the CHC's active catalytic sites, that resulted in a greater PKO conversion yield [38]. Reports on similar studies, as defined by Nath et al. [24] and Olatundun et al. [28], show that soybean and *honne* oil biodiesel yield, respectively, increased as the concentration of catalyst developed from *Brassica nigra* plant and cocoa pod husk-plantain peel blend (CCP) increased. This revealed that catalyst loading has a significant effect on biodiesel yield, and this current result corresponds to those reported in similar studies.

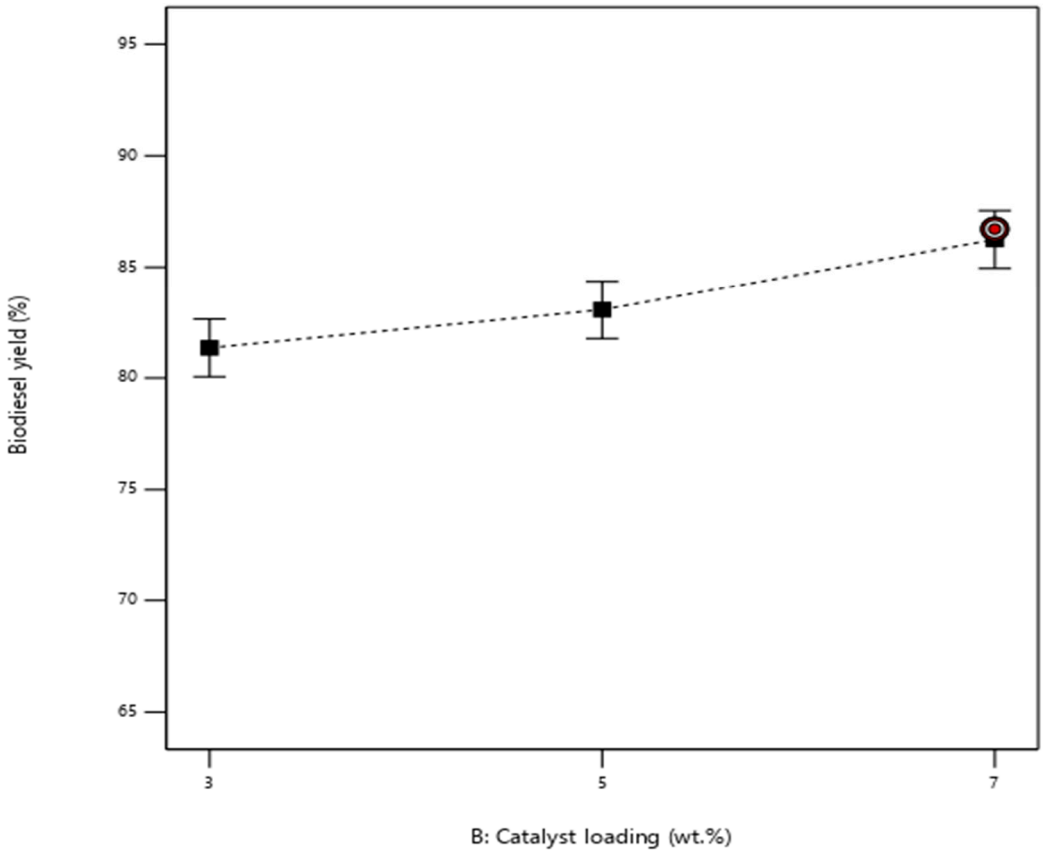

Figure 11. Impact of catalyst loading on PKOEE yield using the selected CHC.

4.7.3. Impact of Reaction Temperature on PKOEE Yield Obtained Using the Selected CHC

The influence of reaction temperature on the PKOEE yield was studied at various temperatures (45 °C to 65 °C) using the developed CHC. The other optimum process variables were maintained (an ethanol-to-oil ratio of 6:1, 7.0 wt.% catalyst loading, and a reaction time of 120 min). As shown in Figure 12, biodiesel yield decreased from 82.86% to 76.9% as reaction temperature increased from 45 °C to 55 °C, then increased significantly to 86.45 wt.%. It has been discovered that an increase in reaction temperature can improve the mass transfer of reactants and the dispersion of the catalyst particles [34]. Hence, the behaviour of the PKOEE yield in relation to reaction temperature may be linked to an increase in the reactant-molecule collision, resulting in increased PKOEE production. Nath et al. [24] found a similar tendency when transesterifying soybean oil with calcined *Brassica nigra* plant ash as a catalyst. A decrease in biodiesel yield from 98.87% to 98.79% was

reported as reaction temperature increased from 32 to 65 °C. Likewise, Olatundun et al. [28] reported comparable behavior with reaction temperature in the transesterification of *honne* oil conversion. As such, our findings fit with other similar works. The optimal yield (86.45%) was observed at the reaction temperature of 65 °C, thus making it the optimum temperature employed for further investigation in this study.

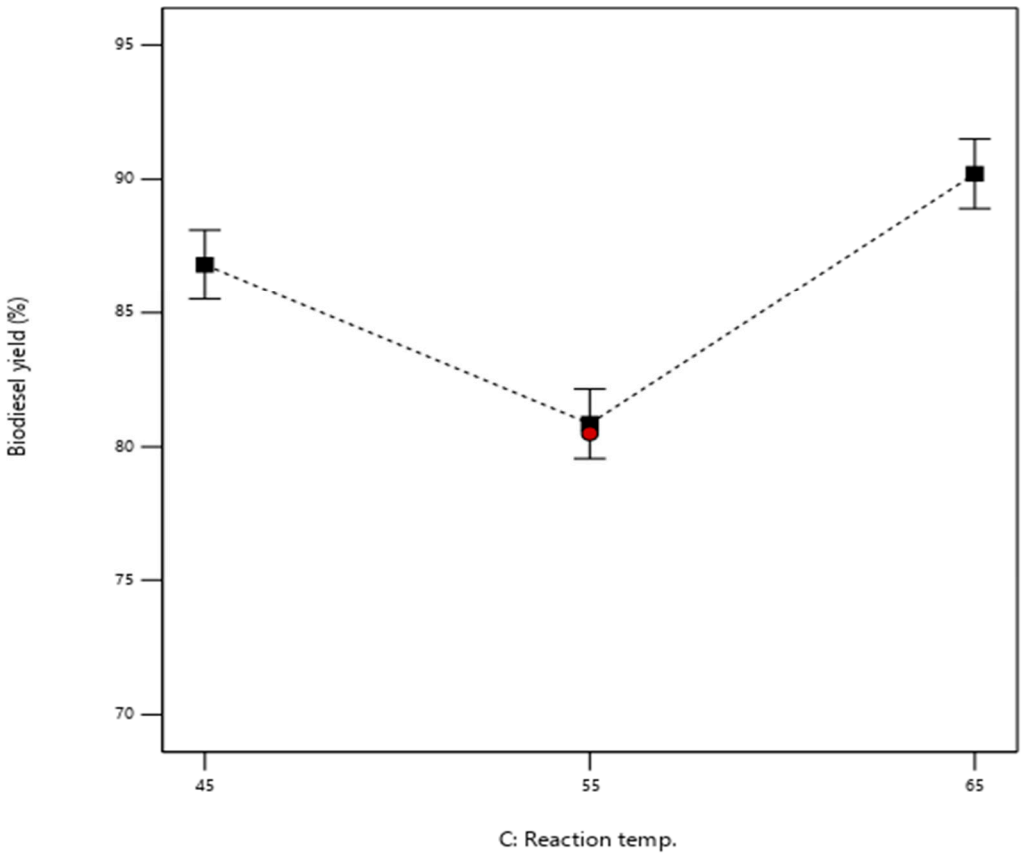

Figure 12. Impact of reaction temperature on PKOEE yield using the selected CHC.

4.8. Catalyst Stability via Reusability Studies Obtained Using the Selected CHC

The reusability ability of the CHC was investigated by using the catalyst for four consecutive reaction cycles under the previously determined optimum reaction conditions. For the reusability investigation of CHC, the approach described by Nath et al. [24], Falowo et al. [3], and Oloyede et al. [10] was used. The product mixture and the catalyst were separated by filtration through Whatman filter paper at the end of each transesterification cycle (110 microns). The CHC was reapplied without any additional treatment, such washing or calcination. Figure 13 depicts the biodiesel (PKOEE) yield for the four consecutive cycles. According to the graph, the CHC attained a maximum biodiesel yield of 86.72% in the first run and a yield of 82.12% in the fourth. The decreased activity of the recovered catalyst after each cycle could be attributed to the deactivation of active basic sites as a result of the loss of particular elements, which can reduce the active sites of a catalyst [34]. The results showed that the catalyst had excellent reusability efficiency, possibly attributable to the inclusion of transition metal oxides in the catalyst [54].

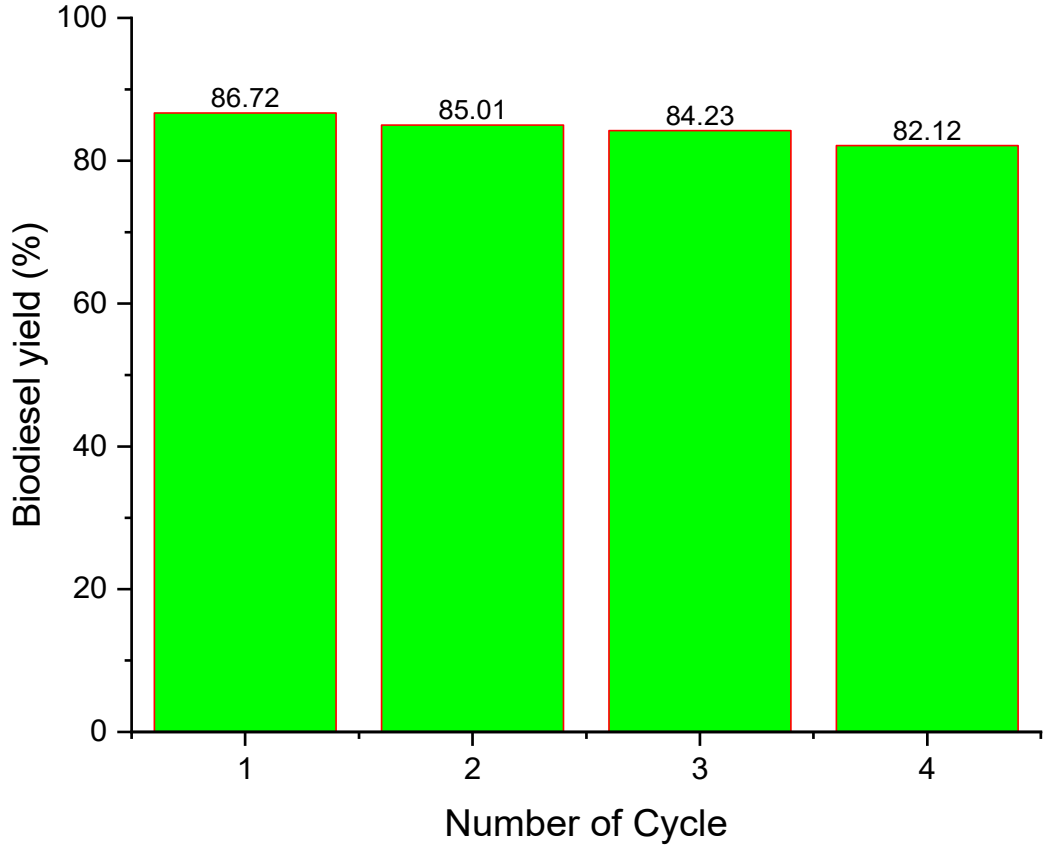

Figure 13. Catalyst reusability vs PKOEE yield obtained using the selected CHC.

4.9. Relationship between the Structure and Catalytic Performance of CHC

The developed CHC underwent thermal decomposition via calcination at 800 °C, resulting in the formation of oxides responsible for the catalyst's catalytic performance. The newly developed CHC was used to catalyze the transesterification of PKO. The developed CHC's catalytic performance during transesterification is primarily attributed to the ionic reaction between the cations and anions in the structural phases of Ca^{2+}-O^{2-}, Mg^{2+}-CO_3^{2-}, and Si^{4+}–O^{2-} in the CHC. As a result, these components are thought to be the primary catalytic sites for PKO's catalyzed transesterification reaction. The activity of the oxide of Ca^{2+} and Mg^{2+} in transesterification reactions for several calcined ash derived heterogeneous base catalysts has been reported by Oloyede et al. [2]. The CHC stability during reusability may also be due to the formation of Ca–O bond and bond of C=O and CO groups of CO_3^{2-} in the CHC. A similar relationship was reported for the CaO–MoO_3–SBA–15 composite heterogeneous catalyst developed by Xie and Zhao [16].

5. Fatty Acid Compositions of PKOEE

The fatty acid compositions of PKOEE produced using the developed CHC for transesterification of PKO are described in Table 13. The major ethyl esters found in the product were ethyl esters of dodecanoate (25.4%), 2-elaidate (20.3%), decanoate (15.2%), 9-hexadecadienoate (11.6%), octadecanoate (10.5%), tetradecanoate (7.5%), and hexadecanoate (4.5%). The results demonstrated that the PKOEE obtained using the CHC had a highly saturated composition, comparable with what has been reported for PKOEE synthesized using CPWSA, CMSHA, and CLBPA as catalysts.

Table 13. Fatty acid composition of PKOEE using the developed CHC.

Composition (wt.%)					
		PKOEE		PKOEE	
		Present Study		Previous Study by the Authors	
Fatty Acid Esters	**Formula**	**CHC**	**CPWSA [8]**	**CMSHA [8]**	**CLBPA [8]**
Saturated fatty acids					
Ethyl behenate	$C_{24}H_{48}O_2$	0.03	0.2	0.1	0.5
Ethyl nonanoate	$C_{11}H_{22}O_2$	0.02	ND	0.06	0.6
Ethyl octanoate	$C_{10}H_{20}O_2$	2.86	3.96	3.93	3.95
Ethyl hexadecanoate	$C_{18}H_{36}O_2$	4.5	0.83	0.85	0.78
Ethyl tetracosanoate	$C_{26}H_{52}O_2$	0.10	0.09	0.08	0.08
Ethyl decanoate	$C_{12}H_{24}O_2$	15.2	1.5	2.3	1.9
Ethyl pentadecanoate	$C_{17}H_{34}O_2$	0.9	1.2	1.1	2.1
Ethyl dodecanoate	$C_{14}H_{28}O_2$	25.4	38.6	36.3	44.05
Ethyl octadecenoate	$C_{20}H_{40}O_2$	10.5	8.5	7.3	8.01
Ethyl tetradecanoate	$C_{16}H_{32}O_2$	7.5	0.6	2.3	0.95
Unsaturated fatty acids					
Ethyl 2-hexdecanoate	$C_{16}H_{30}O_2$	0.5	NP	NP	NP
Ethyl elaidate	$C_{20}H_{38}O_2$	20.3	43.05	45.21	35.9
Ethyl-9-hexadecenoate	$C_{18}H_{34}O_2$	11.6	0.43	0.07	0.19
Ethyl-9,12-octadecadienoate	$C_{20}H_{36}O_2$	0.56	0.9	NF	1.3

[NF]: Not discovered, [NP]: Not published.

6. Conclusions

This study demonstrated the feasibility of creating a biobased Composite Heterogeneous Catalyst (CHC) from three blended agricultural residues (periwinkle shell, melon seed husk, and locust bean pod-husk) for sustainable biodiesel synthesis. The catalytic strength of the new CHC was tested by catalyzing the transesterification of PKO with ethanol to produce PKOEE. The catalyst's chemical, structural, and morphological components were investigated. The Taguchi method was used to optimize the transesterification process. The Taguchi Orthogonal Array design was used to obtain the best potential combinations of transesterification process variables. The investigation resulted in the following finding:

I. Using SLDM, the optimal ratio for synthesizing CHC was discovered to be 66.7% (PWSP) and 16.7% (MSHP and LBPP, respectively). The catalyst contains 69.049% Ca and 9.472% K in their elemental form and 61.592% CaO and 7.919% K_2O in their oxide form, as well as other transition elements in their elemental and oxide forms.
II. The surface area, pore volume, and pore size of the catalyst were determined to be 215. 5.3 m^2g^{-1}, 0.4903 cm^3g^{-1}, and 2.022 nm (20.220 Å), respectively, using the BET technique. The presence of a mesopore is indicated in the catalyst. As a result, the CHC is a mesoporous nanomaterial. SEM revealed an agglomeration of non-uniform particles with a spongy microporous shape.
III. The optimum conditions for catalyzed transesterification processes (EtOH-to-PKO ratio of 12:1, CHC loading of 7%, 65% reaction temperature, and reaction time of 40 min) demonstrated that the proposed catalysts could yield more than 90% PKOEE.
IV. The authors claim that the yield and purity of PKOEE obtained using the synthesized composite catalyst are superior to those obtained using each of the residues separately.

V. The PKOEE produced using CHC satisfied the ASTM D6751 and EN 14214 standard conditions.

As a result, the feasibility of developing a biobased composite heterogeneous base catalyst for sustainable biodiesel synthesis using a blend of peri-winkle shells, melon seed husk, and locust bean pod husk was demonstrated.

Author Contributions: Conceptualization, C.T.O. and A.O.A. (Abass Olanrewaju Alade); Data curation, C.T.O. and O.O.; Formal analysis, C.T.O., A.O.A. (Abass Olanrewaju Alade) and O.O.; Investigation, C.T.O. and A.O.A. (Ademola Oyejide Adebayo); Methodology, C.T.O., A.O.A. (Abass Olanrewaju Alade) and A.I.A.; Project administration, S.O.J., O.O. and C.T.O.; Resources, O.T.L., G.F.S. and I.M.R.F.; Software, O.O., O.T.L., A.O.A. (Ademola Oyejide Adebayo) and C.T.O.; Supervision, S.O.J. and O.T.L.; Validation, S.O.J. and O.O.; Visualization, A.O.A. (Abass Olanrewaju Alade), A.O.A. (Ademola Oyejide Adebayo) and A.I.A.; Writing—original draft, C.T.O., A.O.A. (Abass Olanrewaju Alade), O.O. and I.M.R.F.; Writing—review and editing, I.M.R.F., G.F.S., O.O. and C.T.O. All authors have read and agreed to the published version of the manuscript.

Funding: There is no funding received for this research.

Data Availability Statement: The data presented in this study are available on request from the corresponding author.

Acknowledgments: The second author (Simeon Olatayo Jekayinfa) thanks the Alexander von Humboldt Foundation in Germany for the Equipment Subsidy award, which greatly aided the outcome of this work.

Conflicts of Interest: The authors declare no conflict of interest.

References

1. Ogunkunle, O.; Ahmed, N.A. A review of global current scenario of biodiesel adoption and combustion in vehicular diesel engines. *Energy Rep.* **2019**, *5*, 1560–1579. [CrossRef]
2. Oloyede, C.T.; Jekayinfa, S.O.; Alade, A.O.; Ogunkunle, O.; Otung, N.-A.U.; Laseinde, O.T. Exploration of agricultural residue ash as a solid green heterogeneous base catalyst for biodiesel production. *Eng. Rep.* **2022**, *5*, e12585. [CrossRef]
3. Falowo, O.A.; Ojumu, T.V.; Pereao, O.; Betiku, E. Sustainable Biodiesel Synthesis from Honne-Rubber-Neem Oil Blend with a Novel Mesoporous Base Catalyst Synthesized from a Mixture of Three Agrowastes. *Catalysts* **2020**, *10*, 190. [CrossRef]
4. Sarin, A. *Biodiesel: Production and Properties*; Royal Society of Chemistry: London, UK, 2012.
5. Razzaq, L.; Mujtaba, M.A.; Soudagar, M.E.M.; Ahmed, W.; Fayaz, H.; Bashir, S.; Fattah, I.M.R.; Ong, H.C.; Shahapurkar, K.; Afzal, A.; et al. Engine performance and emission characteristics of palm biodiesel blends with graphene oxide nanoplatelets and dimethyl carbonate additives. *J. Environ. Manag.* **2021**, *282*, 111917. [CrossRef]
6. Betiku, E.; Okeleye, A.A.; Ishola, N.B.; Osunleke, A.S.; Ojumu, T.V. Development of a Novel Mesoporous Biocatalyst Derived from Kola Nut Pod Husk for Conversion of Kariya Seed Oil to Methyl Esters: A Case of Synthesis, Modeling and Optimization Studies. *Catal. Lett.* **2019**, *149*, 1772–1787. [CrossRef]
7. Hoang, A.T.; Ong, H.C.; Fattah, I.M.R.; Chong, C.T.; Cheng, C.K.; Sakthivel, R.; Ok, Y.S. Progress on the lignocellulosic biomass pyrolysis for biofuel production toward environmental sustainability. *Fuel Process. Technol.* **2021**, *223*, 106997. [CrossRef]
8. Fattah, I.M.R.; Ong, H.C.; Mahlia, T.M.I.; Mofijur, M.; Silitonga, A.S.; Rahman, S.M.A.; Ahmad, A. State of the Art of Catalysts for Biodiesel Production. *Front. Energy Res.* **2020**, *8*, 101. [CrossRef]
9. Mofijur, M.; Masjuki, H.H.; Kalam, M.A.; Atabani, A.E.; Fattah, I.M.R.; Mobarak, H.M. Comparative evaluation of performance and emission characteristics of *Moringa oleifera* and Palm oil based biodiesel in a diesel engine. *Ind. Crop. Prod.* **2014**, *53*, 78–84. [CrossRef]
10. Tunji Oloyede, C.; Olatayo Jekayinfa, S.; Olanrewaju Alade, A.; Ogunkunle, O.; Timothy Laseinde, O.; Oyejide Adebayo, A.; Veza, I.; Fattah, I.M.R. Potential Heterogeneous Catalysts from Three Biogenic Residues toward Sustainable Biodiesel Production: Synthesis and Characterization. *Chemistryselect* **2022**, *7*, e202203816. [CrossRef]
11. Mofijur, M.; Siddiki, S.Y.A.; Shuvho, M.B.A.; Djavanroodi, F.; Fattah, I.M.R.; Ong, H.C.; Chowdhury, M.A.; Mahlia, T.M.I. Effect of nanocatalysts on the transesterification reaction of first, second and third generation biodiesel sources—A mini-review. *Chemosphere* **2021**, *270*, 128642. [CrossRef]
12. Nsair, A.; Onen Cinar, S.; Alassali, A.; Abu Qdais, H.; Kuchta, K. Operational Parameters of Biogas Plants: A Review and Evaluation Study. *Energies* **2020**, *13*, 3761. [CrossRef]
13. Falowo, O.A.; Oladipo, B.; Taiwo, A.E.; Olaiya, A.T.; Oyekola, O.O.; Betiku, E. Green heterogeneous base catalyst from ripe and unripe plantain peels mixture for the transesterification of waste cooking oil. *Chem. Eng. J. Adv.* **2022**, *10*, 100293. [CrossRef]
14. Semwal, S.; Arora, A.K.; Badoni, R.P.; Tuli, D.K. Biodiesel production using heterogeneous catalysts. *Bioresour. Technol.* **2011**, *102*, 2151–2161. [CrossRef] [PubMed]

15. Suryaputra, W.; Winata, I.; Indraswati, N.; Ismadji, S. Waste capiz (*Amusium cristatum*) shell as a new heterogeneous catalyst for biodiesel production. *Renew. Energy* **2013**, *50*, 795–799. [CrossRef]
16. Xie, W.; Zhao, L. Heterogeneous CaO–MoO3–SBA-15 catalysts for biodiesel production from soybean oil. *Energy Convers. Manag.* **2014**, *79*, 34–42. [CrossRef]
17. Ramachandran, K.; Sivakumar, P.; Suganya, T.; Renganathan, S. Production of biodiesel from mixed waste vegetable oil using an aluminium hydrogen sulphate as a heterogeneous acid catalyst. *Bioresour. Technol.* **2011**, *102*, 7289–7293. [CrossRef]
18. Aleman-Ramirez, J.L.; Moreira, J.; Torres-Arellano, S.; Longoria, A.; Okoye, P.U.; Sebastian, P.J. Preparation of a heterogeneous catalyst from moringa leaves as a sustainable precursor for biodiesel production. *Fuel* **2021**, *284*, 118983. [CrossRef]
19. Aleman-Ramirez, J.; Okoye, P.U.; Torres-Arellano, S.; Paraguay-Delgado, F.; Mejía-López, M.; Moreira, J.; Sebastian, P.J. Development of reusable composite eggshell-moringa leaf catalyst for biodiesel production. *Fuel* **2022**, *324*, 124601. [CrossRef]
20. Tan, Y.H.; Abdullah, M.O.; Nolasco-Hipolito, C. The potential of waste cooking oil-based biodiesel using heterogeneous catalyst derived from various calcined eggshells coupled with an emulsification technique: A review on the emission reduction and engine performance. *Renew. Sustain. Energy Rev.* **2015**, *47*, 589–603. [CrossRef]
21. Betiku, E.; Odude, V.O.; Ishola, N.B.; Bamimore, A.; Osunleke, A.S.; Okeleye, A.A. Predictive capability evaluation of RSM, ANFIS and ANN: A case of reduction of high free fatty acid of palm kernel oil via esterification process. *Energy Convers. Manag.* **2016**, *124*, 219–230. [CrossRef]
22. Onoji, S.E.; Iyuke, S.E.; Igbafe, A.I.; Daramola, M.O. Transesterification of Rubber Seed Oil to Biodiesel over a Calcined Waste Rubber Seed Shell Catalyst: Modeling and Optimization of Process Variables. *Energy Fuels* **2017**, *31*, 6109–6119. [CrossRef]
23. Etim, A.O.; Betiku, E.; Ajala, S.O.; Olaniyi, P.J.; Ojumu, T.V. Potential of Ripe Plantain Fruit Peels as an Eco-friendly Catalyst for Biodiesel Synthesis: Optimization by Artificial Neural Network Integrated with Genetic Algorithm. *Sustainability* **2018**, *10*, 707. [CrossRef]
24. Nath, B.; Das, B.; Kalita, P.; Basumatary, S. Waste to value addition: Utilization of waste Brassica nigra plant derived novel green heterogeneous base catalyst for effective synthesis of biodiesel. *J. Clean. Prod.* **2019**, *239*, 118112. [CrossRef]
25. Miladinović, M.R.; Zdujić, M.V.; Veljović, D.N.; Krstić, J.B.; Banković-Ilić, I.B.; Veljković, V.B.; Stamenković, O.S. Valorization of walnut shell ash as a catalyst for biodiesel production. *Renew. Energy* **2020**, *147*, 1033–1043. [CrossRef]
26. Adebayo, A.O.; Jekayinfa, S.O.; Agbede, O.O.; Oloyede, C.T.; Kolade, A.I.; Ademola, H. Biogas Production Potential of Moringa (*oleifera* L.) Residues at Mesophilic Temperature. *Am. J. Eng. Res.* **2020**, *9*, 87–92.
27. Oloyede, C.T.; Akande, F.B.; Oniya, O.O. Moisture dependent physical properties of sour-sop (*Annona muricata* L.) seeds. *Agric. Eng. Int. CIGR J.* **2015**, *17*, 185–190.
28. Olatundun, E.A.; Borokini, O.O.; Betiku, E. Cocoa pod husk-plantain peel blend as a novel green heterogeneous catalyst for renewable and sustainable honne oil biodiesel synthesis: A case of biowastes-to-wealth. *Renew. Energy* **2020**, *166*, 163–175. [CrossRef]
29. Oloyede, C.T.; Akande, F.B.; Oriola, K.O.; Oniya, O.O. Thermal properties of soursop seeds and kernels. *Res. Agric. Eng.* **2017**, *63*, 79–85. [CrossRef]
30. Okoye, C.C.; Okey-Onyesolu, C.F.; Nwokedi, I.C.; Eije, O.C.; Asimobi, E.I. Biodiesel Synthesis from Waste Cooking Oil Using Periwinkle Shells as Catalyst. *J. Energy Res. Rev.* **2020**, *4*, 32–43. [CrossRef]
31. Wang, W.; Cheng, Y.; Tan, G.; Tao, J. Analysis of Aggregate Morphological Characteristics for Viscoelastic Properties of Asphalt Mixes Using Simplex Lattice Design. *Materials* **2018**, *11*, 1908. [CrossRef]
32. Okoye, P.U.; Wang, S.; Xu, L.; Li, S.; Wang, J.; Zhang, L. Promotional effect of calcination temperature on structural evolution, basicity, and activity of oil palm empty fruit bunch derived catalyst for glycerol carbonate synthesis. *Energy Convers. Manag.* **2019**, *179*, 192–200. [CrossRef]
33. Dhawane, S.H.; Kumar, T.; Halder, G. Biodiesel synthesis from *Hevea brasiliensis* oil employing carbon supported heterogeneous catalyst: Optimization by Taguchi method. *Renew. Energy* **2016**, *89*, 506–514. [CrossRef]
34. Yusuff, A.S.; Adeniyi, O.D.; Olutoye, M.A.; Akpan, U.G. Development and Characterization of a Composite Anthill-chicken Eggshell Catalyst for Biodiesel Production from Waste Frying Oil. *Int. J. Technol.* **2018**, *9*, 291–319. [CrossRef]
35. Kumar, R.S.; Sureshkumar, K.; Velraj, R. Optimization of biodiesel production from *Manilkara zapota* (L.) seed oil using Taguchi method. *Fuel* **2015**, *140*, 90–96. [CrossRef]
36. Karmakar, B.; Dhawane, S.H.; Halder, G. Optimization of biodiesel production from castor oil by Taguchi design. *J. Environ. Chem. Eng.* **2018**, *6*, 2684–2695. [CrossRef]
37. Kolakotia, A.; Setiyo, M.; Rochman, M.L. A green heterogeneous catalyst production and characterization for biodiesel production using RSM and ANN approach. *Int. J. Renew. Energy Dev.* **2022**, *11*, 703–712. [CrossRef]
38. Oladipo, B.; Betiku, E. Optimization and kinetic studies on conversion of rubber seed (*Hevea brasiliensis*) oil to methyl esters over a green biowaste catalyst. *J. Environ. Manag.* **2020**, *268*, 110705. [CrossRef]
39. Pathak, G.; Das, D.; Rajkumari, K.; Rokhum, S.L. Exploiting waste: Towards a sustainable production of biodiesel using *Musa acuminata* peel ash as a heterogeneous catalyst. *Green Chem.* **2018**, *20*, 2365–2373. [CrossRef]
40. Rajkumari, K.; Das, D.; Pathak, G.; Rokhum, S.L. Waste-to-useful: A biowaste-derived heterogeneous catalyst for a green and sustainable Henry reaction. *New J. Chem.* **2019**, *43*, 2134–2140. [CrossRef]
41. Li, B.; Chen, G.; Zhang, H.; Sheng, C. Development of non-isothermal TGA–DSC for kinetics analysis of low temperature coal oxidation prior to ignition. *Fuel* **2014**, *118*, 385–391. [CrossRef]

42. Nair, P.; Singh, B.; Upadhyay, S.; Sharma, Y. Synthesis of biodiesel from low FFA waste frying oil using calcium oxide derived from *Mereterix mereterix* as a heterogeneous catalyst. *J. Clean. Prod.* **2012**, *29–30*, 82–90. [CrossRef]
43. Falowo, O.A.; Oloko-Oba, M.I.; Betiku, E. Biodiesel production intensification via microwave irradiation-assisted transesterification of oil blend using nanoparticles from elephant-ear tree pod husk as a base heterogeneous catalyst. *Chem. Eng. Process. Process. Intensif.* **2019**, *140*, 157–170. [CrossRef]
44. Balajii, M.; Niju, S. A novel biobased heterogeneous catalyst derived from *Musa acuminata* peduncle for biodiesel production–Process optimization using central composite design. *Energy Convers. Manag.* **2019**, *189*, 118–131. [CrossRef]
45. Gohain, M.; Laskar, K.; Phukon, H.; Bora, U.; Kalita, D.; Deka, D. Towards sustainable biodiesel and chemical production: Multifunctional use of heterogeneous catalyst from littered *Tectona grandis* leaves. *Waste Manag.* **2020**, *102*, 212–221. [CrossRef] [PubMed]
46. Ogunkunle, O.; Oniya, O.O.; Adebayo, A.O. Yield Response of Biodiesel Production from Heterogeneous and Homogeneous Catalysis of Milk Bush Seed (*Thevetia peruviana*) Oil. *Energy Policy Res.* **2017**, *4*, 21–28. [CrossRef]
47. Odude, V.O.; Adesina, A.J.; Oyetunde, O.O.; Adeyemi, O.O.; Ishola, N.B.; Etim, A.O.; Betiku, E. Application of Agricultural Waste-Based Catalysts to Transesterification of Esterified Palm Kernel Oil into Biodiesel: A Case of Banana Fruit Peel Versus Cocoa Pod Husk. *Waste Biomass Valorization* **2019**, *10*, 877–888. [CrossRef]
48. Akhabue, C.E.; Okwundu, O.S. Monitoring the transesterification reaction of castor oil and methanol by ultraviolet visible spectroscopy. *Biofuels* **2017**, *10*, 729–736. [CrossRef]
49. Aladetuyi, A.; Olatunji, G.A.; Ogunniyi, D.S.; Odetoye, T.E.; Oguntoye, S.O. Production and characterization of biodiesel using palm kernel oil; fresh and recovered from spent bleaching earth. *Biofuel Res. J.* **2014**, *4*, 134–138. [CrossRef]
50. Akhabue, C.E.; Ogogo, J.A. Modelling and optimization of transesterification of palm kernel oil catalyzed by calcium oxide derived from hen eggshell wastes. *Ife J. Sci.* **2018**, *20*, 127–138. [CrossRef]
51. Olutoye, M.A.; Adeniyi, O.D.; Yusuff, A.S. Synthesis of Biodiesel from Palm Kernel Oil Using Mixed Clay-Eggshell Heterogeneous Catalysts. *Iran. J. Energy Environ.* **2016**, *7*, 308–314.
52. Saravanakumar, A.; Avinash, A.; Saravanakumar, R. Optimization of biodiesel production from Pungamia oil by Taguchi's technique. *Energy Sources Pt A Recover. Util. Environ. Eff.* **2016**, *38*, 2524–2529. [CrossRef]
53. Dhawane, S.H.; Karmakar, B.; Ghosh, S.; Halder, G. Parametric optimization of biodiesel synthesis from waste cooking oil via Taguchi approach. *J. Environ. Chem. Eng.* **2018**, *6*, 3971–3980. [CrossRef]
54. Mansir, N.; Teo, S.H.; Rabiu, I.; Taufiq-Yap, Y.H. Effective biodiesel synthesis from waste cooking oil and biomass residue solid green catalyst. *Chem. Eng. J.* **2018**, *347*, 137–144. [CrossRef]